Tada et al. Progress in Earth and Planetary Science (2016) 3:4
DOI 10.1186/s40645-016-0080-y

Progress in Earth and Planetary Science
a SpringerOpen Journal

REVIEW Open Access

Evolution and variability of the Asian monsoon and its potential linkage with uplift of the Himalaya and Tibetan Plateau

Ryuji Tada[1*], Hongbo Zheng[2] and Peter D. Clift[3]

Abstract

Uplift of the Himalaya and Tibetan Plateau (HTP) and its linkage with the evolution of the Asian monsoon has been regarded as a typical example of a tectonic–climate linkage. Although this linkage remains unproven because of insufficient data, our understanding has greatly advanced in the past decade. It is thus timely to summarize our knowledge of the uplift history of the HTP, the results of relevant climate simulations, and spatiotemporal changes in the Indian and East Asian monsoons since the late Eocene. Three major pulses of the HTP uplift have become evident: (1) uplift of the southern and central Tibetan Plateau (TP) at ca. 40–35 Ma, (2) uplift of the northern TP at ca. 25–20 Ma, and (3) uplift of the northeastern to eastern TP at ca. 15–10 Ma. Modeling predictions suggest that (i) uplift of the southern and central TP should have intensified the Indian summer monsoon (ISM) and the Somali Jet at 40–35 Ma; (ii) uplift of the northern TP should have intensified the East Asian summer monsoon (EASM) and East Asian winter monsoon (EAWM), as well as the desertification of inland Asia at 25–20 Ma; and (iii) uplift of the northeastern and eastern TP should have further intensified the EASM and EAWM at 15–10 Ma. We tested these predictions by comparing them with paleoclimate data for the time intervals of interest. There are insufficient paleoclimate data to test whether the ISM and Somali Jet intensified with the uplift of the southern and central TP at 40–35 Ma, but it is possible that such uplift enhanced erosion and weathering that drew down atmospheric CO_2 and resulted in global cooling. There is good evidence that the EASM and EAWM intensified, and desertification started in inland Asia at 25–20 Ma in association with the uplift of the northern TP. The impact of the uplift of the northeastern and eastern TP on the Asian monsoon at 15–10 Ma is difficult to evaluate because that interval was also a time of global cooling and Antarctic glaciation that might also have influenced the intensity of the Asian monsoon.

Keywords: East Asian summer monsoon, East Asian winter monsoon, Indian summer monsoon, Himalaya, Tibetan Plateau, Chinese Loess Plateau, Climate model, Tectonic–climate linkage, Westerly jet, Desertification

Review

The East Asian monsoon and its importance

The Asian monsoon is the largest and strongest monsoon system in the world. Although monsoon is a regional phenomenon driven by the heat contrast between the continent and the ocean, it is so large that its behavior exerts a significant influence on the global climate. The Asian monsoon is divided into three subcomponents, the South Asian (or Indian) monsoon, the Southeast Asian monsoon, and the East Asian monsoon (EAM), although the Southeast Asian monsoon may not be as closely linked to the Himalaya and Tibetan Plateau (HTP) as the other two.

The EAM is one of the major components of the Asian monsoon system and is thus an integral part of the global climate system. It is subdivided into the East Asian summer monsoon (EASM) and East Asian winter monsoon (EAWM). The EASM controls the hydrological cycle in East Asia, where over one third of the global population resides. Thus, its economic and social impact is profound. It also exerts a significant impact on

* Correspondence: ryuji@eps.s.u-tokyo.ac.jp
[1]Department of Earth and Planetary Science, Graduate School of Science, The University of Tokyo, 7-3-1 Hongo, Bunkyo-ku, Tokyo 113-0033, Japan
Full list of author information is available at the end of the article

Springer

© 2016 Tada et al. **Open Access** This article is distributed under the terms of the Creative Commons Attribution 4.0 International License (http://creativecommons.org/licenses/by/4.0/), which permits unrestricted use, distribution, and reproduction in any medium, provided you give appropriate credit to the original author(s) and the source, provide a link to the Creative Commons license, and indicate if changes were made.

the global carbon cycle through its role in controlling chemical weathering, as well as the burial of organic carbon (Raymo and Ruddiman 1992; France-Lannord and Derry 1997; Hren et al. 2007). EASM precipitation and EAWM winds affect the oceanography of East Asian marginal seas through controlling nutrient input and the salinity balance (e.g., Tada et al. 1999; Tada 2004; Kubota et al. 2010, 2015), together with upwelling and deep-water ventilation (e.g., Tada et al. 1999; Itaki et al. 2004; Ikehara and Itaki 2007). As a result, it is important to understand how the EAM evolved through time and identify the major controls on its evolution.

Some researchers claim that the EAM is not a typical monsoon because it is not simply driven by the thermal contrast between the continent and ocean, but is affected by the topography of Tibet (e.g., Molnar et al. 2010). However, since this review focuses on the potential linkage between the HTP uplift and evolution of the Asian monsoon, we particularly focus on the EAM because its evolution is expected to have been closely linked to the topographic development of the HTP.

The EAM system

The EASM is driven by the sea level pressure contrast between the Asian Low and the Pacific High (Zhao and Zhou 2009) and is characterized by a seasonally migrating precipitation front (the Meiyu–Baiu Front) that appears in Southeast Asia in May, gradually migrates northwest during early summer, and disappears in August (Sampe and Xie 2010) (Fig. 1). Its seasonal northeast migration is considered to be influenced by the westerly jet (WJ) that passes to the south of the Himalaya during winter and to the north of Tibet from early May to October (Schiemann et al. 2009). Sampe and Xie (2010) demonstrated that the WJ axis over China bounds the northern limit of Meiyu–Baiu Front, and its northward migration is the cause of the northwest migration of the front over East Asia during the early summer. Yanai and Wu (2006) provide a thorough review of the thermal and dynamical influences of the HTP on the Asian monsoon and WJ.

In contrast, the EAWM is driven by the thermal contrast between the Asian continent and the North Pacific Ocean during winter when the Siberian High develops over the Asian continent and the Aleutian Low develops in the North Pacific. However, recent studies suggest that the contrast between the Asian continent and the Maritime Continent is also important (e.g., Wang and Chen 2014). The EAWM is characterized by dry and cold northwesterly, northerly, and northeasterly winds that blow from the Siberian High toward the Aleutian Low and a low pressure system that develops over the Maritime Continent (MC)–northern Australia region north of the equator during winter (MC Low) (Chang et al. 2006). A strong EAWM is characterized by stronger Siberian High–Aleutian Low and/or MC Low pressure contrasts, stronger low-level northwesterly winds along the Russian coast, a deeper mid-tropospheric trough, and an enhanced upper level WJ (Jhun and Lee 2004). The intensity of the EASM is defined as $I_{EAWM} = (2 \times SLP_1^* - SLP_2^* - SLP_3^*) / 2$ where SLP_1^*, SLP_2^*, and SLP_3^* indicate the normalized average sea level pressure over Siberia (40–60° N, 70–120° E), the North Pacific (30–50° N, 140–170° W), and the Maritime Continent (20S–10° N, 110–160° E), respectively (Wang and Chen 2014). It is important to note that the EAWM in the Maritime Continent–northern Australia region and Southeast Asia (e.g., Vietnam and Malaysia) is characterized by northeasterly winds and a wet climate.

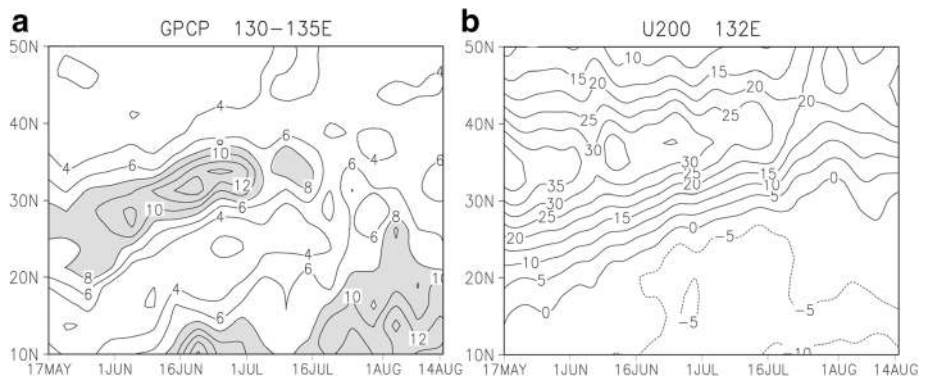

Fig. 1 Latitude–time sections of (**a**) GPCP precipitation and (**b**) 200 hPa westerly wind at 132° E. *GPCP* (Global Precipitation Climatology Project) precipitation averaged at 130–135° E (contours are 2 mm day^{-1}, shaded for values >8 mm day^{-1}) (**a**), and 200 hPa westerly wind at 132° E (every 5 m s^{-1}) (**b**) shows the seasonal march of the summer monsoon front and the westerly jet axis over East Asia. It is evident that the position of the westerly jet axis bounds the northern limit of the EASM front position. Adopted from Sampe and Xie (2010)

Conceptual basis for the HTP uplift–Asian Monsoon intensification hypothesis

As will be discussed in more detail in the next section, the effects of large-scale mountains, such as the HTP, on global and regional climates were explored during early stages of climate model development (e.g., Manabe and Terpstra 1974; Hahn and Manabe 1975). Results from climate model simulations suggest that the strong intensity of the current Asian monsoon and dryness in inland Asia are due mainly to the presence of the Tibetan Plateau (TP) (e.g., Kutzbach et al. 1989; Ruddiman and Kutzbach 1989; Manabe and Broccoli 1990; Broccoli and Manabe 1992). As a result, the HTP uplift–Asian monsoon intensification hypothesis has been attracting long-lived interest of geoscientists from all over the world since this was first proposed. The presence of the HTP is thought to strengthen the Asian monsoon in three ways (e.g., Ruddiman and Prell 1997).

The first mechanism is enhancement of the heat contrast caused by the altitude of the TP. The high altitude of the TP and the thinner atmosphere above it allow the surface temperature of the plateau to increase during summer. As a result, the surface temperature of the TP becomes higher than the temperature of the surrounding air at the same altitude. This temperature contrast causes advection of air above the plateau, which is responsible for the formation of a low-pressure cell over the TP during summer and thus intensifies the Asian summer monsoon (Manabe and Terpstra 1974; Webster et al. 1998). In contrast, extensive snow cover on the plateau during winter causes excess cooling of the plateau.

The second influence of the HTP on the Asian monsoon is the rain shadow effect of the Himalaya. Because vigorous advection occurs above the TP, strong seasonal airflow occurs from the Indian Ocean toward the TP. This flow crosses the 7000 m high Himalayan mountain chain, which acts as a geomorphological barrier to air advection. Warm and moist air flowing from the Indian Ocean toward the advection center on the TP has to ascend the frontal slopes of the Himalaya and is cooled adiabatically, expelling moisture as precipitation. This process causes high precipitation along the frontal slopes of the Himalaya, releases heat, and enhances the uplift of dry air masses, thereby further strengthening advection.

The third process associated with the effect of the HTP on the Asian monsoon is the topographic barrier effect of the TP that forces the WJ to take two discrete routes over Asia (Fig. 2a, b). The core altitude of the WJ is ca. 10 km, but it can reach 5 km at its lowest limit. Consequently, the HTP acts as a topographic barrier for the WJ and forces it to take two discrete routes: one along the southern margin of the Himalaya and the other to the north of the TP (Ono et al. 1998; Tada 2004; Nagashima et al. 2007; 2011). Meteorological observations reveal that the WJ flows along the southern margin of the Himalaya during winter months and then suddenly jumps to the north of the TP in May and stays there until late September when it switches back to the south of the Himalaya (Schiemann et al. 2009; Fig. 2b). Meteorological observations also show that the Meiyu–Baiu Front suddenly appears in association with a jump of the WJ axis to the north of the TP in May and migrates northward in association with the northward shift of the WJ axis (Schiemann et al. 2009; Sampe and Xie 2010). The WJ axis bounds the northern limit of the Meiyu–Baiu Front in East Asia (Sampe and Xie 2010). Thus, the topographic barrier effect of the HTP causes a significant northward migration of the WJ during the summer that allows northwestward penetration of the summer monsoon front into East Asia.

In addition to these "direct" effects of the HTP uplift on the Asian monsoon, Raymo et al. proposed that late Cenozoic global cooling was caused by enhanced physical and chemical weathering and consequent draw down of atmospheric CO_2 triggered by the uplift of the HTP (Raymo et al. 1988; Raymo and Ruddiman 1992). This global cooling might, in turn, have influenced the long-term evolution of the Asian monsoon.

Remaining problems

Although there is a sound theoretical basis to expect that the HTP uplift is one of the major causes driving the establishment of the modern state of Asian monsoon, the HTP uplift–Asian monsoon intensification hypothesis is still not proven after ~40 years of ongoing research. One of the major reasons hampering the testing of this hypothesis is that the timing and mode of surface uplift in different parts of the HTP is poorly constrained and still controversial. Controversy has arisen, especially between those approaching this problem from the southern side of the HTP (dominantly European and American scientists) and those approaching from the northern side of the HTP (dominantly Chinese scientists). The former group tends to consider the major phase of the HTP uplift to be older than the Miocene (e.g., Tapponnier et al. 2001; Harris 2006; Rowley and Currie 2006; Royden et al. 2008), whereas the latter group tends to suggest that the major uplift phase occurred in the Plio-Pleistocene (e.g., An et al. 2001; Qiang et al. 2001). However, this controversy has been gradually settled thanks to the introduction of low-temperature thermochronometers and the accumulation of chronostratigraphic and thermochronological data from across the HTP region, as well as

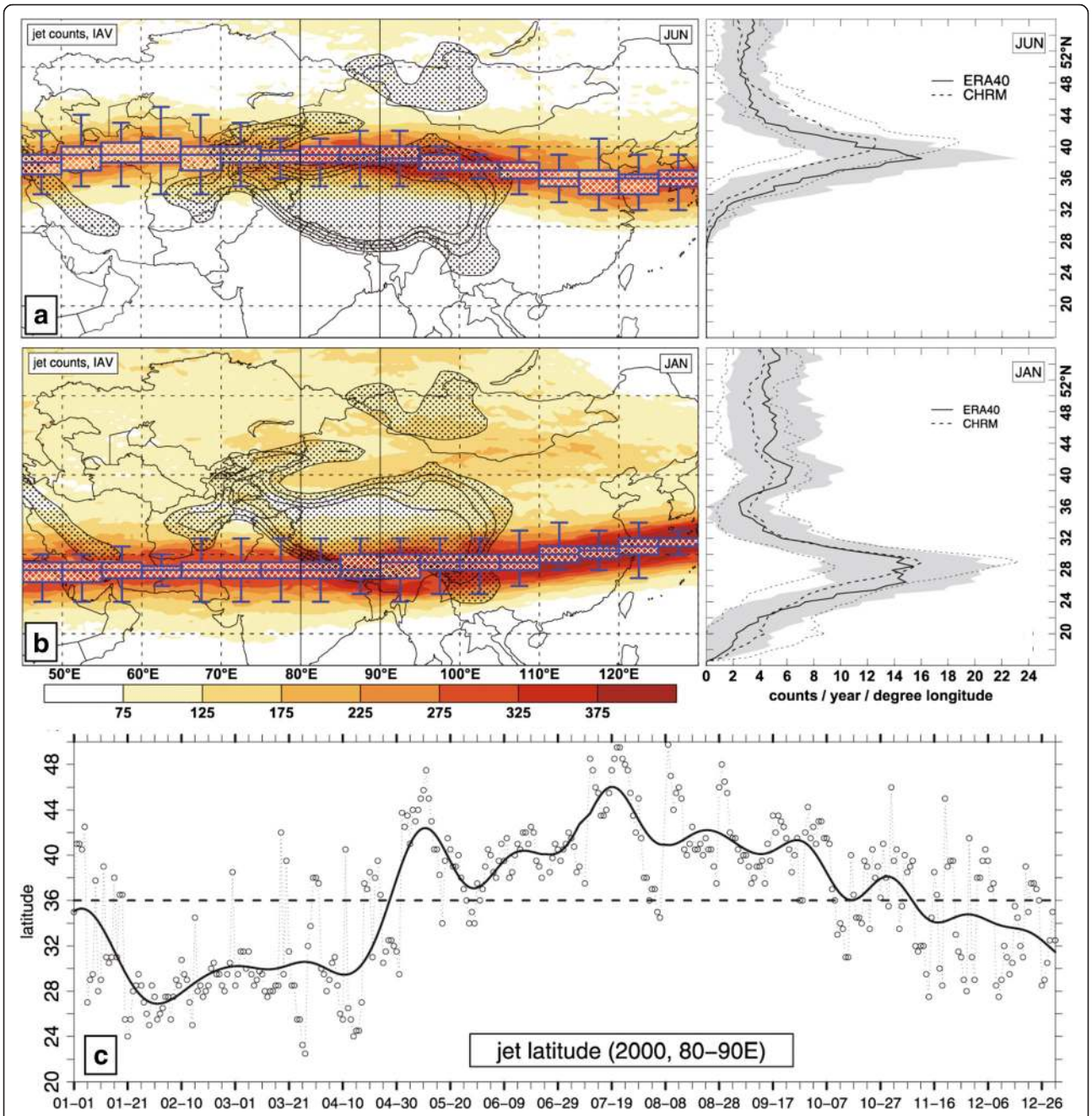

Fig. 2 Seasonal changes of the westerly jet axis over the Tibetan Plateau at approximately 200 hPa. **a** is for June, and **b** is for January. Figures on the left show total jet occurrence counts (*shading*) from 6-h ERA-40 fields and the interannual variability of the jet latitude (box plots) from ERA-40 monthly mean horizontal wind. Figures on the *right* show the meridional distribution of occurrence counts from 80–90° E; i.e., within the area marked by *solid vertical lines*. The *bold solid line* and *gray shading* in the figures on the *right* show the mean and one standard deviation of interannual variability, respectively. **c** is the seasonal cycle of the daily jet latitude at 80–90° E (*open circles*) and the jet latitude obtained after low-pass filtering with a cutoff period of 30 days (*solid line*). Modified from Schiemann et al. (2009)

progress in paleoaltimetry studies during the last decade (e.g., Whipp et al. 2007; Quade et al. 2011).

Another factor that hampered testing the hypothesis is problems with incorporating HTP topography into climate models at sufficient resolution because of limited computing speeds. The ability of climate models to incorporate high-resolution topography has been improved significantly with continuous advance in the performance of supercomputers, which has enabled modelers to test the sensitivities of South Asian and East Asian monsoons to the uplift in the different parts of the HTP (Zhang et al. 2012a; Liu and Dong 2013).

Compared with the impressive progresses in our understanding of the uplift history of the HTP and in climate model simulations of the evolution of the Asian monsoon in response to the uplift of the HTP, advancement in our understanding of the evolution of South Asian (i.e., Indian) and East Asian monsoons has been rather limited. This lack of progress is primarily because relatively few new marine cores have been available for paleoclimate studies on the Asian monsoons; there were no Ocean Drilling Program (ODP)/Integrated Ocean Drilling Program (IODP) cruises between the winter of 1999, when Leg 184 drilled the South China Sea (Wang et al. 2000), and the summer of 2013, when the IODP Expedition 346 drilled the Japan Sea and the northern tip of the East China Sea (Tada et al. 2015). Following Expedition 346, a series of expeditions were conducted to focus on the Asian Monsoon, including Expeditions 353 (Indian Monsoon Rainfall), 354 (Bengal Fan), 355 (Arabian Sea Monsoon), and 359 (Maldives Monsoon and Sea Level). These new expeditions will greatly advance our understanding of the evolution of the Asian monsoon.

Objectives and strategy of this review

Starting with Expedition 346 in the summer of 2013, the IODP has continued to conduct a series of expeditions in the northwest Pacific and Indian Oceans to study the Asian monsoon. As a result, significant numbers of new cores are becoming available to the paleoclimatic/paleoceanographic community. It is thus timely to refresh and update our knowledge concerning the evolution and variability of the Asian monsoon and its potential linkage with the HTP uplift.

The objectives of this review are threefold. In the next section, we summarize the history and recent advances in climatic model simulations that explore the relationship between the uplift of the HTP and the evolution of the Asian monsoon. In the third section, we summarize the timing and mode of the uplift of various parts of the HTP during the Cenozoic based on a number of different types of geological evidence. In the fourth section, we summarize the evolution of the EAM during the Cenozoic. By combining climate model results described in the second section with the uplift history of the HTP reconstructed from geological evidence described in the third section, we predict how the uplift of different parts of the HTP has impacted the nature and intensity of the Asian monsoon. In the fifth section, the predicted results are compared with paleoclimatic reconstructions of the evolution of the Asian monsoon described in the fourth section and the validity of the predictions is discussed.

Evaluating the effects of the HTP uplift on the evolution of the Asian monsoon based on climate models

Early climate model studies (whole TP uplift)

Many climate model simulations have tried to evaluate the effect of the HTP uplift on the intensity of the Asian monsoon. The history of model studies is summarized by Liu and Dong (2013). Manabe et al. initiated climate model studies of the effects of the HTP uplift on the Asian monsoon in the early 1970s (Manabe and Terpstra 1974; Hahn and Manabe 1975), about a decade after the development of general circulation models (GCMs). They used an atmospheric GCM (AGCM) with prescribed insolation and sea surface temperature (SST) and compared simulation results with and without mountains to explore the effects of topography on global atmospheric circulation and climate. They found that HTP topography is essential to the development of both the Siberian High during the boreal winter and Indian summer monsoon (ISM) circulation to the south of the TP during the boreal summer. However, the earliest GCMs had low spatial resolution, did not incorporate sophisticated physical, chemical, and biological processes, and were not well tuned with observational data (Liu and Dong 2013).

GCMs have drastically improved with the rapid increase in computational power since the 1970s and have become capable of conducting higher-resolution simulations and incorporating more processes and many different boundary conditions. From the late 1980s, efforts to compare simulation results with paleoclimate records were initiated by Kutzbach et al. who conducted sensitivity experiments prescribed with full-mountains, half-mountains, and no-mountains and compared simulated results with geological data to constrain tectonically driven surface uplift and climate change. They used an AGCM with orbital parameters, atmospheric pCO_2, SST, sea ice and snow cover, land albedo, and soil moisture to conduct more detailed estimates of climate sensitivity to progressive mountain uplift (Kutzbach et al. 1989; Ruddiman and Kutzbach 1989). They concluded that the presence of the TP intensifies Asian summer and winter monsoons through enhanced summer heating and winter cooling over the plateau, which leads to amplification of the seasonal contrast, as well as from the topographic effect of the TP on the WJ and surface winds (Kutzbach et al. 1989). They proposed that the uplift of the TP may have played an important role in the initiation of northern hemisphere glaciations, although its effect alone falls far short of explaining the full amplitude of Cenozoic cooling (Ruddiman and Kutzbach 1989; Ruddiman et al. 1989). Manabe and Broccoli (1990) also explored the role of mountains in maintaining extensive arid climates in the middle latitudes of the northern hemisphere (see also Broccoli and

Manabe 1992) and stressed the importance of orographically induced stationary wave troughs.

Stepwise uplift of global topography was further pursued by Kitoh et al. (Kitoh 2002, 2004; Abe et al. 2003, 2004), who used an atmosphere–ocean coupled GCM (CGCM) with T42 (ca. 2.8° longitude) resolution, which can reproduce the monsoon and El Niño Southern Oscillation (ENSO) without flux adjustments, to study the sensitivity of the Asian summer monsoon, formation of the Meiyu–Baiu rainband, and changes in the tropical and subtropical atmosphere–ocean system in response to progressive mountain uplift. They found that the Indian, Southeast Asian, and East Asian summer monsoons behaved differently with progressive uplift. Whereas continuous and accelerated intensification is observed for the ISM, the intensity becomes strongest at 40 % uplift for the Southeast Asian monsoon and 80 % for EASM (Abe et al. 2003). They also predicted the formation of the Meiyu–Baiu rainband at 60 % uplift and a switch in the moisture source from the Indian Ocean to the Pacific Ocean (Kitoh 2004). With progressive mountain uplift, the following occurs in the tropical to subtropical Pacific: the Western Pacific warm pool appears, the east–west equatorial SST gradient increases, and the Pacific subtropical anticyclone, associated trade winds, and the Kuroshio Current become stronger (Kitoh 2002, 2004; Abe et al. 2004). They also compared CGCM and AGCM results, finding that the CGCM showed a greater sensitivity to mountain uplift than the AGCM, and stressed the importance of using CGCMs for robust climate modeling.

Around the same time, Liu and Yin (2002) conducted stepwise uplift experiments for the TP using an AGCM with ca. 7.5° longitude resolution coupled with a vegetation model. They found that evolution of the EAM is more sensitive than the Indian monsoon to the uplift of the TP. They stressed that intensification of the EAWM is more significant than that of the EASM and that there seems to be a threshold at ca. 50 % uplift after which the Siberian High becomes distinct and the EAWM is established (Fig. 3). Desertification in inland Asia also occurs during later phases of the TP uplift. On the other hand, summer monsoon-like circulation exists in India and Southeast Asia even without the TP. The uplift of the TP slightly increases the intensity of Indian and Southeast Asia monsoons in early phases, but their intensities gradually decrease in later phases. Different evolutionary processes are thus predicted in response to the uplift of the TP for the Indian, Southeast Asian, and Northeast Asian summer monsoons. This conclusion is similar to that of Abe et al. (2003), but the timing of intensification with respect to the uplift of the TP is different between the two studies. This difference is partly a result of different summer monsoon intensity indices used by the two studies and perhaps also because the model used by Abe et al. (2003) includes air–sea coupling.

Results of these simulations reveal that the uplift of the TP intensifies Asian monsoons. However, the evolution of monsoons in response to the uplift of the TP is different for India, Southeast Asia, and Northeast Asia, and also between summer and winter. It is also suggested that there could be thresholds in the TP uplift for the development of Asian monsoons. However, it is not necessarily clear what kinds of mechanisms are responsible for intensification of each regional and seasonal aspects of the Asian monsoon and which parts of the orography are critical for such mechanisms.

Subsequent climate model studies (partial HTP uplift)

Since the late 2000s, simulation studies began to focus more on mechanisms for monsoon intensification and the effects of the uplift on different parts of the HTP at different times. This research direction reflected the realization that the plateau was not uplifted as a single block at a single time. For example, Chakraborty and Srinivasan (2006) examined the effect of different parts of global orography on the onset timing of the ISM using seasonal simulations with different orographic initial conditions from an AGCM with T-80 (ca. 1.4°) resolution. They found that initiation of the ISM is greatly affected by the orography of the western Himalaya that

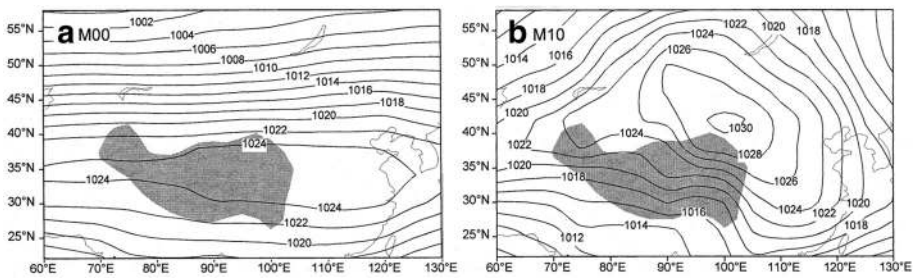

Fig. 3 Change in position and intensity of the Siberian High with the uplift of the TP. The figure is based on an AGCM experiment by Liu and Yin (2002). Winter average SLP distributions for **a** no mountain and **b** full mountain experiments are shown (unit: hPa). Modified from Liu and Yin (2002)

acts as a barrier to cold winds from upper latitudes. Because the intensity of rainfall is not affected by orography after onset of the ISM, the timing of the ISM is the main control on ISM rainfall intensity.

Following this result, Boos and Kuang (2010) challenged the conventional view that the TP acts as a thermal source that induces convection and enhances the ISM. They noticed that upper-tropospheric temperatures peak not in the center but south of the TP during the boreal summer and that the Tibetan High is also centered south of the TP. Based on this observation, they proposed that thermal forcing from continental India (south of the Himalaya) may be more important than that from the TP in controlling the ISM. In this scenario, the Himalaya plays a role in insulating high-entropy, warm, and moist tropical air over India from low-entropy, cold, and dry air from the extra-tropics. To test this idea, they conducted climate simulations with an AGCM with prescribed modern-day SST and orography; the TP was removed but the Himalaya and adjacent mountain ranges were kept intact, and all surface elevations were set to zero. They found that, except for a reduction in rainfall over the southern Himalaya and East Asia, large-scale ISM circulation is unaffected by removal of the TP provided that the high but narrow orography of the Himalaya and adjacent mountains is preserved. They claimed that it is not the thermal forcing of the TP but the insulating effect of Himalayas that produces ISM circulation. Although their simulation results demonstrate that the presence of the wide TP is not essential for ISM circulation, it is debated whether the insulation effect of the Himalaya is really the main driver of the ISM (Wu et al. 2012a; Boos and Kuang 2013, Chen et al. 2014).

Wu et al. (2012b) criticized the experimental design of Boos and Kuang (2010) because it did not separate the insulating effect of the Himalaya and adjacent mountains from surface sensible heating. Using an AGCM with prescribed seasonally varying SST and sea ice, changing orography, and with and without surface sensible heating on the Iranian Plateau, TP, and Himalaya, they demonstrated that the ISM disappears over northeastern India and the EASM weakens when Himalayan topography is included but surface sensible heating is excluded from the model. This study claimed that thermal forcing rather than the insulating effect is responsible for ISM precipitation, especially over northeastern India.

Boos and Kuang (2013) admitted that their earlier (Boos and Kuang 2010) experiment did not separate the insulating effect from sensible heating, but maintained that the thermal insulating effect is still important to monsoon development. Chen et al. (2014) further reexamined the insulating effect of the TP (and Himalaya) using a CGCM with ca. 2.5° longitude resolution and changing orography. Models were run with the full TP, only the southern margin of TP, and no TP. Similar to Wu et al. (2012a), they concluded that diabatic heating in the mid-troposphere along the southern edge of the TP (called candle heating) is more important than the insulating (i.e., blocking) effect (Fig. 4). They demonstrated the importance of the TP for increasing precipitation in East Asia and along the southern and eastern margins of the TP, which is in agreement with other studies. They also showed that the TP plays an important role in reducing precipitation over areas affected by the Somali Jet in northern India and Southeastern Asia. Aside from work by Abe et al. (2003), this effect had not been observed in other experiments. The difference was attributed by Boos and Kuang (2013) to the usage of a CGCM that allows atmosphere–ocean interactions, such as the strong upwelling and reduction in SST that leads to intensification of the Somali Jet, which in turn reduces precipitation in areas affected by the Somali Jet in northern India and Southeastern Asia.

Recent climate model studies (phased HTP uplift)

Although consensus has not yet been reached about the mode and timing of the uplift of the HTP, recent progress in thermochronological and paleoaltimetrical studies on the HTP uplift has allowed climate modelers to estimate the sequence and ages of the HTP uplift. Zhang et al. (2012b) used an AGCM with 1.9° longitude resolution with prescribed SST and sea ice cover to examine the effects of climate on the uplift of the HTP. Based on the idea that the TP was gradually uplifted from south to north, they assumed that the central–southern TP was uplifted first, followed by the Himalaya, the northern TP, and then the Mongolian Plateau. They designed five numerical experiments with different topographies and showed an increase in summer precipitation over the TP and the development of cyclonic circulation anomalies in response to the uplift of the central–southern TP. Their results also demonstrated the importance of the uplift of the Himalaya and northern TP to the evolution of the ISM and EASM, respectively. In particular, the uplift of the Himalaya strengthens summer 850 hPa winds off the Arabian coast (Somali Jet) and enhances summer precipitation in South Asia (northeastern Arabian Sea and central–southern India), as well as the southwestern margin of the Himalaya. On the other hand, the uplift of the northern TP strengthens the western North Pacific subtropical high, intensifies EASM circulation, and enhances summer precipitation in northern East Asia. They also showed decreasing precipitation in central Asia in response to the uplift of the northern TP. These results are in general agreement with those of Boos and Kuang (2010) and Chen et al.

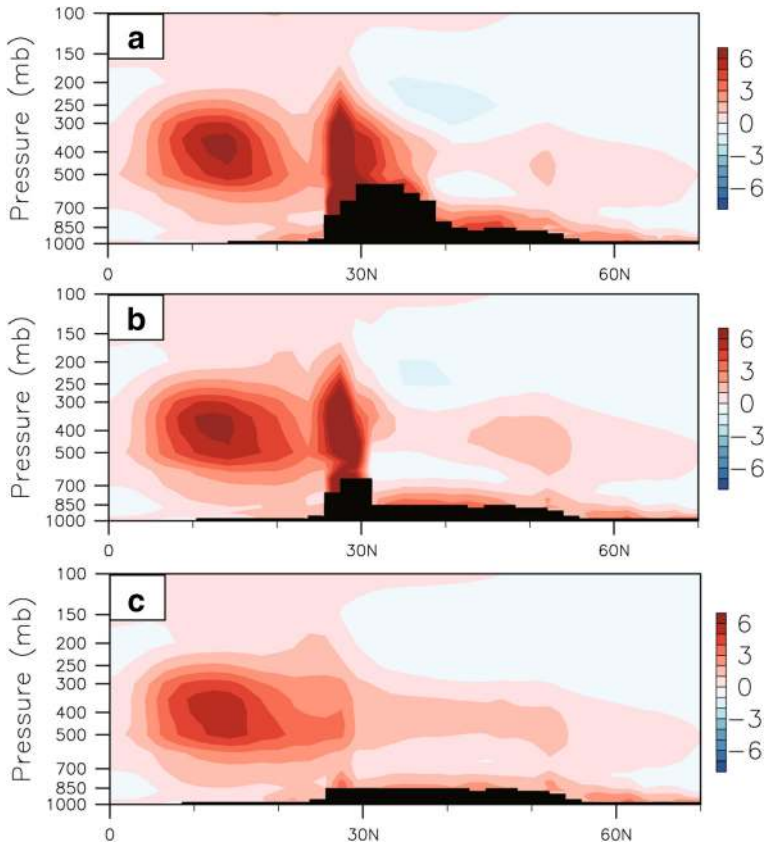

Fig. 4 Meridional cross sections of total diabatic heating (K day^{-1}) averaged between 85 and 95° E. They are based on experiments with **a** the full TP, **b** the narrow southern TP, and **c** no TP. In **b** and **c**, the no-TP parts are set to 1200 m. The *black shaded region* denotes the topography in the experiment. It should be noted that only the uplift of the southern margin of TP is enough to cause diabatic heating along the frontal Himalaya and/or the southern margin of the TP. From Chen et al. (2014)

(2014), suggesting robust connections between the Himalayan uplift and ISM intensification, as well as the northern TP uplift and EASM intensification (Fig. 5).

Tang et al. (2013) conducted sensitivity experiments assuming sequential growth of different parts of Asian orography using a regional climate model with 1 × 1° resolution covering 0°–60° N and 50°–140° E. Boundary conditions other than orography are set to be the same as present in the model, and the model was driven by the output from the present control run and a Late Miocene run performed in the CGCM. They conducted sensitivity experiments with five sequential uplift steps; starting from no mountains (orography higher than 250 m was removed), then the southern TP, central TP, northern TP, Zagros–Hindu Kush–Elburz mountains, and Tien Shan–Altai mountains are added sequentially.

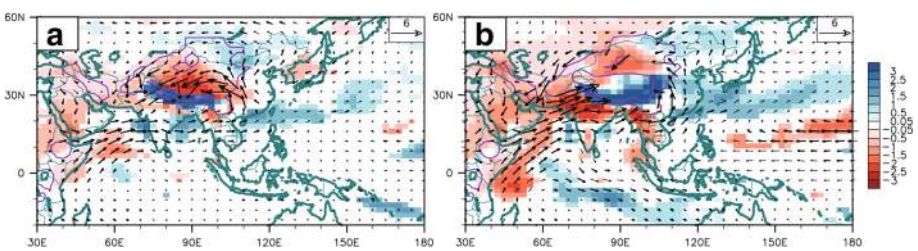

Fig. 5 Differences in surface wind (m s^{-1}) and precipitation (mm day^{-1}) in JJA between the experiments. **a** is the narrow southern TP minus no TP and **b** is full TP minus no TP from Chen et al. (2014) using the Community Earth System Model. *Blue* indicates positive and *red* indicates negative precipitation change. Only significant precipitation values are shown (*color shading*). *Bold vectors* indicate significant changes in wind. *Purple contours* denote elevations of 1200 and 3000 m. Modified from Chen et al. (2014)

They found that the presence of the southern TP and Zagros Mountains greatly enhances ISM wind and precipitation, but reduces EASM wind and precipitation and that the presence of the central and northern TP and the Tien Shan Mountains increases summer precipitation and low-level southerly winds in East Asia, but results in an anticyclonic wind anomaly that suppresses summer precipitation in northern India.

Although these results are in general agreement with previous studies mentioned above (e.g., Boos and Kuang 2010; Zhang et al. 2012a; Chen et al. 2014), they demonstrated the importance of the Zagros Hindu Kush–Elburz mountains for intensification of the Somali Jet and their insulating effect that leads to an increase in summer rainfall in northwestern India. They further argued that the subtropical rain front over East Asia is primarily formed by the confluence of mid-tropospheric westerly flow from the north and south over the TP. They also showed that middle- and low-level westerly flow from the south of the TP is strengthened by the presence of the central and northern TP but suppressed by the Zagros Mountains.

Potential effects of the Paratethys and atmospheric pCO_2 level

Although it is evident that the uplift of the HTP exerts significant influence on the evolution of the Asian monsoon, it does not necessarily mean that other factors such as land–sea distribution, land surface condition, and/or atmospheric pCO_2 are not important (e.g., Charney 1975; Ramstein et al. 1997; Kripalani et al. 2007). For example, Yasunari et al. (2006) evaluated the effect of land surface processes on monsoon systems and the Tropics and concluded that the albedo effect of vegetation substantially increases both evaporation and atmospheric moisture convergence, and thus significantly enhances precipitation in monsoon regions and the Tropics. However, most simulations that evaluate the effect of the HTP uplift on the evolution of the Asian monsoon use near-modern conditions with respect to geographical distribution of lands and seas and greenhouse gas concentrations (Huber and Goldner 2012).

Among the possible geographical influences on the evolution of the Asian monsoon, the presence of the Paratethys sea seems most significant. The Paratethys was a shallow sea covering much of central Asia during the early Paleogene. Ramstein et al. (1997) used an AGCM with a paleogeography of 10 Ma both with and without the TP (although their TP at 10 Ma is smaller and lower than the modern TP) and 30 Ma with and without the Paratethys. The model used present-day insolation, SST, and pCO_2 values to evaluate the effects of the TP and Paratethys on monsoon evolution. The results revealed that the Paratethys acted as a thermal regulator and allowed an oceanic climate to develop over northern Eurasia. Shrinkage of the Paratethys resulted in a continental climate with larger-amplitude annual temperature variations. The enhancement of continental warming during summer as a result of disappearance of the Paratethys increased the thermal gradient between central Asia and the Indian Ocean, leading to an increase in ISM precipitation over the southern flank of the Himalaya (Ramstein et al. 1997). The decrease in the area of the Paratethys also allowed for the development of the Siberian High and thus intensification of the EAWM. Ramstein et al. (1997) concluded that the retreat of the Paratethys played an important role in the evolution of Asian monsoon intensity as did the uplift of the TP.

Because global warming and its impact on human lives are of major concern to the public, and more than two thirds of the world's population lives in areas influenced by the Asian monsoon, there are many studies concerning the impact of increased atmospheric pCO_2 on the Asian monsoon. For example, Christensen et al. (2013) used 20 Coupled Model Intercomparison project Phase 5 (CMIP5) models to show that mean precipitation, the number of extreme rainfall events, and the inter-annual standard deviation of seasonal mean precipitation of the EASM and South Asian monsoon increase with global warming. These results are similar to previous studies (e.g., Kripalani et al. 2007; Kim and Byun 2009). In contrast, global warming-induced weakening of the EAWM has been predicted by CGCMs (Kimoto 2005; Hori and Ueda 2006).

Summary

Although simulations of the effects of the HTP uplift on the Asian monsoon have produced wide-ranging results, common aspects are shared by many model simulations. These include (1) intensification of summer precipitation in East Asia and northern India, (2) desertification of inland Asia, (3) intensification of the Somali Jet offshore from Somalia and the Arabian Peninsula, and (4) intensification of the EAWM. These are considered robust features of the impact of the HTP uplift on Asian monsoon strength. However, the causes of these features were not well understood until recently when modelers started conducting simulations to evaluate the effect of the uplift of different parts of the HTP on intensification of the Asian monsoon and the desertification of inland Asia. In the following, we summarize recent progress in our understanding of the possible effect of the HTP uplift on the above four climate effects associated with the Asian monsoon.

Many climate model simulations suggest that intensification of the ISM is closely linked to the uplift of the Himalaya (or southern Tibet), whereas the EASM is

rather insensitive to the uplift of the Himalaya (Boos and Kuang 2010; Zhang et al. 2012a; Chen et al. 2014) or may even be negatively influenced by this uplift (Tang et al. 2013). Himalayan uplift is also expected to cause an increase in summer precipitation in northern India and intensification of the Somali Jet. The uplift of the Zagros Hindu Kush–Elburz mountains might also have contributed to the intensification of the Somali Jet and the increase in summer rainfall in northwest India (Tang et al. 2013).

Intensification of the EASM is closely linked to the uplift of the northern TP, which enhances summer precipitation in northern East Asia, as well as the southeastern and eastern TP (Zhang et al. 2012a; Tang et al. 2013; Chen et al. 2014), whereas the uplift of the northern TP reduces ISM precipitation in northern India (Boos and Kuang 2010; Zhang et al. 2012a; Chen et al. 2014). The western North Pacific subtropical high may also be strengthened by this uplift (Zhang et al. 2012a). Decreased precipitation in central Asia is expected in response to the uplift of the northern TP (Zhang et al. 2012a). The uplift of the TP may reduce precipitation over the Somali Jet area, northern India, and Southeastern Asia through ocean–atmosphere interactions (Abe et al. 2003; Chen et al. 2014).

Although models that consider the uplift of the whole TP show an increase in the intensity and gradual northward movement of the center of the Siberian–Mongolian High during winter (Liu and Yin 2002), there are no studies to date that deal with the effects that the uplift of different parts of the HTP have on the position and/or intensity of the Siberian High and Aleutian Low, of which pressure difference drives EAWM winds.

The effects of the presence and then shrinkage of the Paratethys on the evolution of the Asian monsoon should also be considered in addition to the effect of the uplift of the HTP, especially during the Paleogene (Ramstein et al. 1997). In addition to these tectonic effects, the impact of changing pCO_2 on Asian monsoon evolution may be significant during the Cenozoic. An increase (decrease) in atmospheric pCO_2 would increase (decrease) EASM precipitation and reduce (enhance) EAWM intensity, at least with modern boundary conditions but also using Eocene boundary conditions (Huber and Goldner 2012). It is worth noting that the polarized effect of pCO_2 on the EASM and EAWM is different from the effect of the HTP uplift on the EASM and EAWM and could be used to differentiate the impacts of the HTP uplift and changing pCO_2.

History of the HTP uplift

Before the Oligocene

It is generally believed that there was an Andean-type volcanic mountain chain of ~4 km high and a few hundreds of kilometers wide along the southern margin of the Eurasian continent before its collision with India (England and Searle 1986; Kapp et al. 2007; Molnar et al. 2010). Recent geological studies show the presence of a >2000 km long Gangdese Magmatic arc (65 to 44 Ma in age) located in the southern part of the Lhasa Block (see Fig. 6a), below which the Tethyan–Indian Oceanic Plate was subducted northward (e.g., Wu et al. 2013; Xu et al. 2013). However, Hetzel et al. (2011) demonstrated that rapid exhumation of up to 6 km in the northern Lhasa block between 65 and 48 Ma formed low-relief surfaces, probably at an altitude close to sea level. Sporopollen assemblages, characterized by a lack of dark needle-leaved trees, from the southern margin of Qiangtang Block (Fig. 6a) also suggest a low-elevation plain with no high mountains present (Wu et al. 2013). Thus, controversy arose as to whether there was a high volcanic mountain chain along the southern margin of the Eurasian continent before the collision.

Recently, Ding et al. (2014) used oxygen isotope paleoaltimetry to show that the Gangdese Magmatic arc attained an elevation of 4500 m by 60 Ma and argued that the low-relief surfaces reported by Hetzel et al. (2011) may represent a low-elevation corridor between the Gangdese Magmatic arc and the Qiangtang Mountains. Furthermore, Caves et al. (2015) showed that the spatio-temporal distribution of paleoprecipitation $\delta^{18}O$ in central to East Asia during the Cenozoic has stayed remarkably constant since 50 Ma, suggesting that the long-standing topography of southern Tibet has continuously blocked southerly moisture incursion and that the subsequent uplift of the TP has had little impact on the climate of central Asia. Thus, it seems very likely that an Andean-type volcanic mountain chain of ~4 km high was present at the southern margin of the Eurasian continent by 60 Ma.

The collision between India and Eurasia started at ca. 55–45 Ma, and the rate of convergence of the two continents decreased significantly after ca. 45 Ma (Molnar et al. 2010). Based on paleoaltimetric studies using oxygen isotope ratios as well as sedimentological evidence, it is thought that the India–Eurasia collision might have caused the uplift of the southern–central TP to an altitude close to that of present at ca. 40 Ma (Rowley and Currie 2006; Wang et al. 2008; Polissar et al. 2009). Recently, Hoke et al. (2014) examined oxygen isotopes from pedogenic carbonates from the southeastern margin of the TP and concluded that the present elevation of ~3.3 km was attained as early as the late Eocene (>40 Ma) in that part of the TP, suggesting extensive early uplift of the southern TP.

Dai et al. (2012) studied the provenance and sedimentological environment of Paleogene fluvial sediments of the Hoh Xil Basin (Fig. 6a) in the north–central TP,

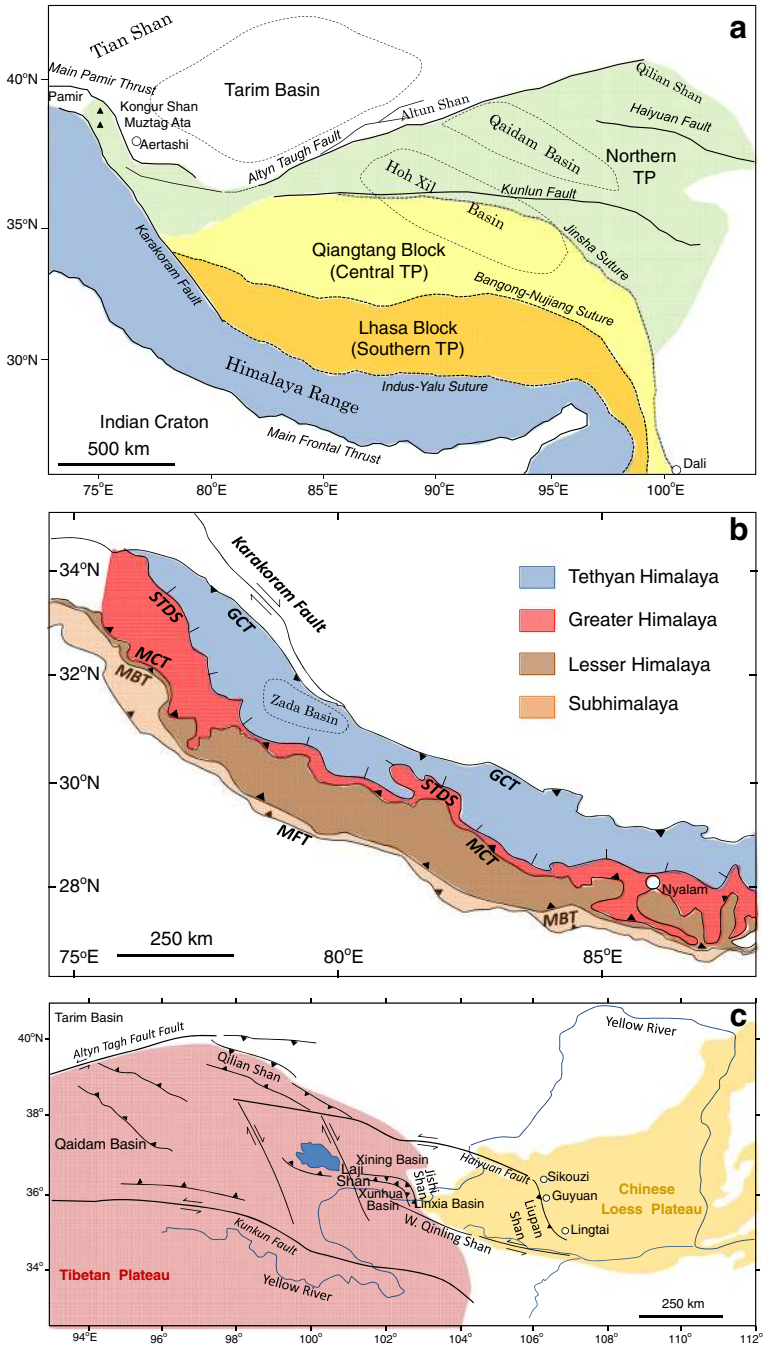

Fig. 6 Tectonic maps of the HTP. **a** covers whole HTP, **b** is a close-up of the Himalayan range, and **c** is a close up of northeastern Tibet and Chinese Loess Plateau, with key geographic features marked

which is more than 500 km wide. They demonstrated that the eastern and western Hoh Xil basins formed a single large foreland basin, and its conglomerate-bearing sediments were derived from the Qiangtang and Lhasa blocks of the central–south TP. These results suggest rapid uplift and erosion of the Qiangtang and Lhasa blocks at ca. 40 Ma.

It is widely believed that the TP gradually grew sequentially north–northeastward as collision continued (e.g., Tapponnier et al. 2001; Wang et al. 2008). This traditional view of northward growth of the TP has recently been challenged by the idea that the northern and southern edges of the TP were already defined and being deformed via the main part of the TP soon after the start

of the collision (Clark 2012; Yuan et al. 2013). Exhumation started at 49–46 Ma, (Yin et al. 2002; Zhu et al. 2006), then accelerated at ca. 45–35 Ma (Clark et al. 2010), and north–south shortening continued until ca. 22 Ma (Yuan et al. 2013) especially in the northeastern TP. Similarly, accelerated exhumation during the middle Eocene (ca. 50–40 Ma) is reported from north–central Pamir (Fig. 6a) and from the Transhimalaya in Ladakh, probably associated with the India–Eurasia collision (Clift et al. 2002; Amidon and Hynek 2010). Furthermore, Dupont-Nivet et al. (2008) examined palynological assemblages of precisely dated lacustrine sediments from Xining Basin (Fig. 6c) in the northeastern TP and found the appearance of high-altitude vegetation at an optimal altitude of 2500–4000 m. This vegetation was possibly derived from West Qinling Shan (Fig. 6c) at 36.1 Ma (magnetic polarity chron C16n2n) (see also Hoorn et al. 2012).

The onset of exhumation ca. 50 Ma at the northern edge of the TP suggests that forces associated with the India–Eurasia collision were transmitted to the northern end of the TP rather rapidly (Clark 2012). However, it is important to note that the onset of deformation at the northern edge of the TP immediately after the India–Eurasia collision and subsequent continuation of deformation does not necessarily mean that the northern part of the TP was uplifted to close to present-day altitudes at that time.

The Oligocene–early Miocene

Thermochronometry shows the temporal acceleration of exhumation between 25 and 20 Ma in the Laji Shan area (Fig. 6c) in the northeastern TP (Lease et al. 2011; Xiao et al. 2012). A similar acceleration in erosion is also reported in the nearby Qilian Shan (Fig. 6a, c) (George et al. 2001) and the Hoh Xil Basin in the north–central TP (Wang et al. 2008). During this period, the orientation of crustal shortening changed from N–S to NE–SW in the northeastern TP (Lease et al. 2011; Yuan et al. 2013). This change in the tectonic deformation mode could be related to the partial removal of the mantle lithosphere under the northern TP and subsequent weakening and outward flowing of the middle to lower crust (Clark and Royden 2000; Royden et al. 2008; Yuan et al. 2013), a process that could have led the TP to reach present-day elevations.

In the northwestern TP and the Pamir Plateau, tectonic deformation and rapid exhumation occurred during the late Oligocene to early Miocene (ca. 25–15 Ma; Sobel and Dumitru 1997; Amidon and Hynek 2010; Zhang et al. 2011). This tectonic event is considered to be the result of the initiation of south-dipping intercontinental subduction between North Pamir and the Tien Shan, which could have been triggered by breaking off of the western end of the north-dipping Indian slab (Sobel et al. 2013). Associated crustal thickening and subsequent partial melting of the lower crust caused extrusion of gneiss domes and rapid exhumation in the central and western Pamir during the late Oligocene to early Miocene (Amidon and Hynek 2010; Thiede et al. 2013). Initiation of the NNW-trending Karakoram Fault (Fig. 6b; right-lateral fault) is also considered to have been associated with the onset of subduction (Thiede et al. 2013).

The 25–15 Ma period is regarded as a transitional period for establishment of a new subduction system (Sobel et al. 2013). Pamir frontal thrusts, such as the Main Pamir Thrust (Fig. 6a), became active during this time (Bershaw et al. 2012). It is thought that the North Pamir was influenced by subduction erosion during the early stages of subduction, but became influenced by subduction accretion by the middle Miocene due to the increasing thickness of sediments involved in the subduction (Sobel et al. 2013). This timing is also similar to (i) slowing of India–Asia convergence rates between 20 and 11 Ma (Molnar and Stock 2009) and (ii) deceleration of strike–slip motion and acceleration of distributed shortening in the northern TP between 18 and 15 Ma (e.g., Ritts et al. 2008).

In the Tibetan and Greater Himalayan regions (Fig. 6b), north–south compression and consequent crustal thickening was active during the early Miocene, as manifested by activation of the Main Central Thrust (MCT) from 22 to 21 Ma, and the Great Counter Thrust (GCT) from 19 to 13 Ma (Fig. 6b) (Murphy et al. 2009), suggesting that this part of the Himalaya reached present-day elevations during this period (Gebelin et al. 2013). The Greater Himalayan sequence, sandwiched between the MCT and Southern Tibetan Detachment System (STDS) (Fig. 6b) and represented by middle- to lower-crustal rocks, is considered to have been extruded from beneath the TP (the channel flow model) (Nelson et al. 1996) during the early to middle Miocene (24–12 Ma) (Catlos et al. 2004). This process is linked to partial melting of the middle–lower crust (Harris 2007). P–T–t paths obtained from the Greater Himalayan Crystalline Series support a 25–23 Ma age for the onset of exhumation (fig. 5 of Harris 2007). Exhumation was particularly vigorous during the Early Miocene (Hodges 2006), most likely due to enhanced erosion caused by focused precipitation (Clift et al. 2008). The Greater Himalayan Sequence was thrusted far to the south over the top of the Lesser Himalaya (Fig. 6b) during this interval (Deeken et al. 2011). Clift et al. (2008) examined the mass accumulation rate of marine sediments from the Indus and Bengal Fan and demonstrated that rates were the highest during middle Miocene when extrusion of Greater Himalayan Sequence was most intense. Clift et al. (2008) further examined chemical weathering indices of marine

sediments from the Indus and Bengal fans to demonstrate that summer monsoon precipitation intensity was higher during this period.

The middle Miocene onward

Thermochronometry data indicate that exhumation of the northeastern TP started at ca. 13 Ma in the Jishi Shan (Fig. 6c) (Lease et al. 2011), at ca. 10 Ma in the Qilian Shan (Zheng et al. 2010), and at ca. 8 Ma in the Liupan Shan (Fig. 6c) (Zheng et al. 2006). Increases in erosion rates and/or grain size and changes in provenance occurred in most of the surrounding basins since ca. 15–10 Ma (Yuan et al. 2013). Recently, Duvall et al. (2013) used low-temperature thermochronometry to examine the timing of the Kunlun and Haiyuan left-lateral faults onset (Fig. 6b) and concluded that exhumation along the western, central, and eastern segments of the Kunlun Fault increased at 12–8, 20–15, and 8–5 Ma, respectively, whereas motion along the Haiyuan Fault started as early as 15 Ma along the western/central segment and 10–8 Ma along the eastern fault tip. Hough et al. (2011) examined the oxygen isotope gradient between Xunhua and Linxia basins across the Jishi Shan and concluded that a rain shadow developed between 16 and 11 Ma, driven by the uplift of the NNW–SSE trending Jishi Shan.

Ritts et al. (2008) studied Oligocene-Miocene clastic sedimentary rocks in the southeastern Tarim Basin in the north–central TP (Fig. 6a). They found planktonic and benthic foraminifer assemblages at the base of orogenic-sourced conglomerate, suggesting temporal intrusion of a shallow sea along the southern margin of the Tarim Basin at that time. They showed that the uplift of the Altun Shan, caused by the oblique reverse faulting of the Northern Altyn Tagh Fault (Fig. 6a), began at 16–15 Ma based on foraminiferal biostratigraphy, correlation of the foraminifera-bearing interval to a global high stand at 15.6 Ma, and reconstruction of the thermal history of the area using two low-temperature thermochronometers. In eastern Pamir, a shallow emplacement of gneiss and subsequent exhumation occurred between 14 and 8 Ma in the north (Muztagh Ata) (Fig. 6a), whereas exhumation occurred from 8 Ma and continues to the present in the south (Kongur Shan) (Fig. 6a) (Thiede et al. 2013).

Along the eastern margin of the TP, southeastward expansion of the plateau started at 13–11 Ma, which probably reflected lower crustal flow toward the southwest (e.g., Clark et al. 2005). Stable isotope paleoaltimetry also suggests that approximately 1 km of post-late-Miocene surface uplift occurred at the southeast margin of the TP to the south of Dali (Hoke et al. 2014), which is consistent with the observations of Clark et al. (2005). It is possible that this late Miocene uplift at the southeastern margin of the TP was also caused by southeastward lower crustal flow. In the southern TP (Lhasa Block), formation of NNE–SSW trending grabens suggesting E–W extension in the plateau interior started as early as 14 Ma and lasted until 4 Ma, based on the dates of fault zone mineralization (e.g., Blisniuk et al. 2001).

In the Tethyan and Greater Himalaya, arc-parallel extension from ca. 14 to 8 Ma resulted in the formation of the huge Zada Basin (Fig. 6b) (Murphy et al. 2009). Paleoaltimetry based on $\delta^{18}O$ in fossil gastropods suggests a 1.0 to 1.5 km decrease in altitude at Zada Basin in the southern TP during the late Miocene (Murphy et al. 2009). It is noteworthy that formation of such basins was coeval with initiation of the Karakorum Fault and its extensions that cut the GCT into the Tethyan Himalayan area (Fig. 6b).

In the frontal Himalaya, extrusion of the Higher Himalayan Crystalline (HHC) thrust sheet onto the Lesser Himalaya (LH) sequence slowed down in the middle Miocene and ceased by ca. 12 Ma (Godin et al. 2006). Based on U–Pb ages of monazite and zircon from the central Himalaya, MCT and STDS activity ceased by 12–13 Ma (Edwards and Harrison 1997; Wu et al. 1998; Catlos et al. 2004). Clift et al. (2008) used the mass accumulation rate of terrigenous sediments in the Indus Fan and probability density analysis of $^{40}Ar/^{39}Ar$ dates of detrital muscovite grains to show that extrusion and erosion of the HHC series seemed to slow down during the late Miocene. The slowing of erosion was interpreted to have been driven by a decrease in ISM precipitation in the frontal Himalaya, possibly due to southward retreat of the ISM front (Huang et al. 2007). Armstrong and Allen (2011) further speculated that this retreat could have been related to the southward shift of the Intertropical Convergence Zone. Approximately synchronous with this event during the middle Miocene, the LH sequence was detached from the under-thrusting Indian plate, thrust under the HHC series, and stacked in the northwestern Himalayan region, thereby forming the Lesser Himalayan Crystalline Complex (Deeken et al. 2011). In the LH, duplexes and thrust sheet stacks were occasionally formed above the mid-crustal ramp, causing growth of the LH from the Middle Miocene to the Early Pliocene (Deeken et al. 2011; Webb et al. 2011). These Lesser Himalayan Crystalline sheets were exhumed after peak metamorphism at ca. 11 Ma (Caddick et al. 2007). Subsequently, deformation propagated southward to the Main Boundary Thrust (MBT) (Fig. 6b), which was activated by 5 Ma (DeCelles et al. 2001; Webb 2013), and then to the Main Frontal Thrust (MFT). Thus, the area of the strongest uplift migrated southward by ca. 100 km within the LH region since ca. 11 Ma. It is noteworthy that a modern precipitation maximum occurs at the

frontal part of the Lesser Himalayan Crystalline sheet, approximately 100 km to the south of the Greater Himalaya in the northwest Himalaya (Deeken et al. 2011).

Although there was a widely held belief that a pulse of tectonic uplift occurred in the northern TP during the Plio-Pleistocene (e.g., An et al. 2001; Tapponnier et al. 2001), recent studies tend to suggest otherwise. For example, many papers that argue for Plio-Pleistocene uplift of the northeastern TP use the onset of fluvial incision of the high-relief plateau margin as a proxy for the timing of the uplift (e.g., Li et al. 1997). However, Craddock et al. (2010) demonstrated that the onset of fluvial incision of the northeastern TP at ca. 1.8 Ma significantly lagged the uplift that occurred in the Middle Miocene. Also, extensive deposition of thick conglomerate beds along the northern margin of the northern TP was used as evidence of Pliocene tectonic uplift of northwestern Tibet (e.g., Zheng et al. 2000). However, our recent reevaluation of the age of the conglomerate beds (the Xiyu Formation) at Aertashi section in southwestern Tarim revealed a deposition onset age of ca. 15 Ma (Zheng et al. 2015). Earlier estimates of the age of the Xiyu Formation and its equivalent conglomerate beds are based solely on magneto-stratigraphy, and so it is necessary to reevaluate their age. There is some evidence of accelerated erosion in the Himalayan region during the Plio-Pleistocene (Huntington et al. 2006). For example, McDermott et al. (2013) suggest an increase in the erosion rate in the area south of STDS at ~3.5 Ma in the Nyalam region in the central Himalaya.

Summary

It is controversial whether an Andean-type high mountain chain already existed before the collision of India with the Eurasian continent (England and Searle 1986; Kapp et al. 2007; Molnar et al. 2010; Hetzel et al. 2011) although recent studies tend to support its existence before collision (Ding et al. 2014; Caves et al. 2015). The first pulse of the HTP uplift in the southern and central TP during the late Eocene (ca. 40 Ma), soon after the "hard" collision of India and Eurasia at ca. 45 Ma, probably resulted in the HTP reaching a height close to that of present (Rowley and Currie 2006; Wang et al. 2008; Polissar et al. 2009; Dai et al. 2012; Hoke et al. 2014). Deformation and exhumation also started at the northern edge of the TP and Pamir soon after the collision and accelerated at ca. 36–35 Ma (Dupont-Nivet et al. 2008; Clark et al. 2010; Hoorn et al. 2012).

A second pulse of surface uplift occurred between 25 and 20 Ma in the northeastern, northwestern, central TP, and Pamir (Sobel and Dumitru 1997; George et al. 2001; Wang et al. 2008; Amidon and Hynek 2010; Lease et al. 2011; Zhang et al. 2011; Xiao et al. 2012). This uplift pulse was extensive and associated with a change in deformation mode, which is interpreted to have been related to the partial removal of mantle lithosphere under the northern TP, and subsequent weakening and thickening of middle to lower crust (Clark and Royden 2000; Royden et al. 2008; Yuan et al. 2013). The Greater Himalayan Sequence was extruded from under the TP and thrust over the LH, a process accompanied by partial melting of the middle to lower crust. Initiation of south-dipping intercontinental subduction occurred between North Pamir and the Tien Shan, which could have been initiated by break-off of the western end of the north-dipping Indian slab (Sobel et al. 2013).

A third pulse of the HTP uplift occurred at around 15 to 10 Ma when the TP expanded toward the north and east to attain a width and altitude close to the present (Hough et al. 2011; Yuan et al. 2013). This event is probably related to the flow of the lower crust due to crustal thickening and northward and eastward expansion of the zone of partial melting under the TP (Clark and Royden 2000; Yuan et al. 2013). It is also suggested that the southernmost part of the HTP became close to the present altitude since 9 to 11 Ma (Rowley and Currie 2006, Saylor et al. 2009) although this may have happened earlier during thrusting of the Greater Himalaya to the south onto the Lesser Himalaya sequence, because modern altitudes are recorded around Mount Everest in the late early Miocene (Gebelin et al. 2013).

After ca. 10 Ma, the uplift continued in the northeastern part of the TP, but this was not as significant as previously thought, whereas progressive southward migration of the zone of greatest rock uplift occurred in the frontal Himalaya (Deeken et al. 2011).

Initiation and evolution of the East Asian monsoon during the Cenozoic

Before the Oligocene

EASM

Latitudinal zonal distribution of climate is considered to have dominated the Paleocene and Eocene in East Asia before the collision of India and Eurasia (Song et al. 1983; Sun and Wang 2005). This climate was thought to be characterized by a subtropical humid zone in the north, a subtropical–tropical and arid–semiarid zone in the middle, and tropical humid zone in the south, with the location of the subtropical high being the main control on this zonal climate distribution (Wang et al. 1999). However, this traditional view was recently challenged by several studies. For example, Quan et al. (2012) examined 66 plant assemblages at 37 localities in China and found that the arid zone proposed in earlier studies experienced relatively high mean annual precipitation of >735 mm. Both western and eastern parts of China had higher mean annual temperatures and precipitation than

central part of China, and the entire area was characterized by rather strong seasonality, suggesting the occurrence of a monsoon climate, especially in the eastern parts of East Asia. This interpretation is supported by the result of sediment facies analysis by Wang et al. (2012), who demonstrated a landward decrease in humidity along an east–west transect in eastern China. Climate model simulations also support the view that the EASM was already active during the Eocene, probably because of higher atmospheric pCO_2 at that time (Huber and Goldner 2012; Zhang et al. 2012a; Licht et al. 2014). However, the monsoon-like climate in East Asia during the Eocene was probably not strong enough to replace the latitudinal arid zone formed by the subtropical high, but only to periodically obscure it by introducing humid air into inland central Asia during the summer (Zhang et al. 2012b).

The Eocene–Oligocene Transition (EOT) at ca. 34 Ma is characterized by a two-step increase in global benthic foraminiferal $\delta^{18}O$ values that reflect the significant growth of Antarctic ice sheets and a temperature decrease in the deep ocean (Lear 2007). Atmospheric CO_2 concentrations are also thought to have decreased over this time (Pearson et al. 2009; Pagani et al. 2011). However, the temporal and casual relationship between the decrease in pCO_2, global cooling, and the build-up of Antarctic ice sheets is not clear because climatic conditions immediately before the EOT are not well documented.

Based on a palynological study of the late Eocene sedimentary succession in the Xining Basin in the northeastern TP, Hoorn et al. (2012) demonstrated that a distinct cooling step occurred at 36.4 Ma (C16r). This step roughly coincides with a distinct decrease in gypsum content at 36.6 Ma (at the top of chron C17n.1n), suggesting that the cooling was accompanied by drying and a decrease in the seasonality of precipitation. It is important to note that a major cooling step preceded the EOT by ca. 2 m.y. and the monsoon-like climate weakened in response to this cooling (Licht et al. 2014).

Desertification

It is critical to identify the timing of onset of desertification in central Asia if we are to assess its possible linkage with the uplift of the HTP. Existing paleoenvironmental records suggest that initial desertification of inland Asia started around the EOT, although the exact age is not well constrained (e.g., Graham Stephan and Yongjun 2005). Dupont-Nivet et al. (2007) used magnetostratigraphy and cyclo-stratigraphy to examine distal alluvial fan deposits from Playa Lake in the northeastern TP. They showed that these deposits are characterized by rhythmical alternations of gypsum and red mudstone layers in the Xining Basin (Fig. 6c) and demonstrated that aridification was accompanied by the disappearance of Playa Lake deposits (gypsum) at the Eocene/Oligocene boundary (EOB) at ca. 33.8 Ma (in the upper part of chron C13r). Because the EOB is marked by an abrupt increase in marine oxygen isotopes that most likely reflects the formation of permanent Antarctic ice sheets, this result suggests a close linkage between global cooling and the aridification of inland Asia.

Subsequent studies of the same sedimentary sequence in Xining Basin revealed three additional phases of aridification before the EOB. Abels et al. (2011) showed that the first phase was characterized by a distinct decrease in gypsum content relative to red mudstone at 36.6 Ma (at the top of chron C17n.1n) and that the second phase was characterized by a substantial increase in the clastic sedimentation rate at 34.7 Ma (at the base of chron C13r). Furthermore, Xiao et al. (2010) demonstrated that the third phase of aridification was characterized by a major reduction in the thickness of the gypsum bed at 34.2 Ma (in the middle of chron C13r). This reduction in gypsum bed thickness coincides with the start of the first shift in marine oxygen isotopes and global cooling (i.e., start of the EOT). Thus, aridification started almost 3 m.y. earlier than the formation of permanent Antarctic ice sheets at the EOB. The occurrence of possible sand dune deposits of approximately EOB age has been reported at the Aertashi section in the southwestern margin of the Tarim Basin (Zheng et al. 2015), indicating an earlier onset of aridification and a possible link with Antarctic glaciation.

The Oligocene–early Miocene

EASM

Paleobotanical and lithological data suggest that the geographic distribution of Oligocene paleoclimatic zones was basically the same in the Oligocene–early Miocene as in the Eocene. However, the data are limited because the distribution of Oligocene sediments are restricted, especially in southeastern China due to the erosion caused by the uplift of the TP (Sun and Wang 2005 2008a; Guo et al. 2008). Nevertheless, a latitudinal zonal pattern, with a less distinct arid zone in the middle latitudes, seems to have lasted throughout the Oligocene (Sun and Wang 2005; Guo et al. 2008).

A drastic change in paleoclimatic patterns occurred around the Oligocene/Miocene boundary (e.g., Sun and Wang 2005; Guo et al. 2008). Based on compilation of paleobotanical and lithological data, Sun and Wang (2005) demonstrated two completely different patterns of climate zonation between the Paleogene and the Neogene. Namely, the latitudinal zonal pattern during the Paleogene changed to a Neogene pattern with arid zones restricted to northwest China. This suggests the

emergence of the EASM at around the beginning of the early Miocene (ca. 23 Ma), when the zonal distribution of arid climate in East Asia was disrupted as a result of the development of a warm and wet climate in eastern China (Sun and Wang 2005; Guo et al. 2008).

This change is also marked by the deposition of "Miocene loess" in the western Chinese Loess Plateau (CLP) started at ca. 22 Ma (Guo et al. 2002). Subsequent studies confirm this finding, showing that loess deposition began in the western CLP as early as 25 Ma, and that stable dry conditions were established by 23 Ma (e.g., Qiang et al. 2011). In the Jungger Basin, approximately 2000 km northwest of the CLP, loess deposition started at ca. 24 Ma and lasted until 8 Ma (Sun et al. 2010a). Recently, Zheng et al. (2015) described the stratigraphy of the Cenozoic sedimentary sequence in the southwestern Tarim Basin using new Ar–Ar and U–Pb ages of pyroclastic beds in the upper part of the sequence. They revised the ages of the underlying Xiyu and Atux Formations, previously thought to have deposited in the Pliocene (Zheng et al. 2000), to be late Oligocene to early Miocene. Based on this new age model, the onset of loess deposition in the Tarim Basin is estimated as ca. 25 Ma (see also Tada et al. 2010). Thus, there is good evidence that the Asian interior (western deserts of China) became drier slightly before the Oligocene/Miocene boundary.

Jiang and Ding (2008) examined the pollen record from fluvio-lacustrine sediments at Guyuan, east of the Liupan Shan (Fig. 6c) in the CLP covering the last 20 Ma and found that the EASM was relatively strong during the early Miocene (20.13–14.25 Ma), although the magnetic susceptibility of loess deposits, commonly used as a summer monsoon proxy in the western CLP (west of Liupan Mountains), is generally low in lower Miocene sediments except between 16 and 14 Ma (Guo et al. 2002; Qiang et al. 2011). A stronger EASM during the early Miocene is also inferred from clay mineral assemblages as well as other geochemical proxies in sediments from the northern South China Sea (Clift et al. 2002; 2014).

Martin et al. (2011) examined the oxygen and carbon isotopes of mammal teeth from a terrestrial sequence in central Pakistan and found relatively high stable $\delta^{18}O$ values between 30 and 22 Ma, suggesting dry conditions. $\delta^{13}C$ values, on the other hand, suggest a C_3-based diet typical of a dense forest and subtropical climate. Palynological data from the surrounding area support this interpretation, but suggest drier habitats occurred later in the Oligocene (De Franceschi et al. 2008). Martin et al. (2011) further reported a gradual (7 ‰) decrease in $\delta^{18}O$ of mammal teeth from central Pakistan from 22 to 15 Ma, which could be partly explained by a global temperature decrease, but more likely reflects the development of a wetter climate. The latter interpretation is consistent with paleobotanical evidence (Antonie et al. 2010), whereas $\delta^{13}C$ values are similar to those during the Oligocene, suggesting the continued dominance of C_3 vegetation. These results suggest intensification of the ISM from 22 to 15 Ma.

EAWM

Eolian dust, accumulated in the CLP (and neighboring marginal seas), is thought to have originated from the Mongolian Gobi desert and been delivered by EAWM winds (e.g., Chen and Li 2013). Thus, the 10–70 μm fraction of detrital material or detrital quartz in loess–paleosol and Red Clay sequences are commonly used as a proxy for wind intensity. Various studies have reconstructed changes in the EAWM during the last 20 Ma (Chen et al. 2006; Sun et al. 2008a; Jiang et al. 2008; Sun et al. 2010b, 2006). For example, Jiang and Ding (2010) examined the 10–70 μm fraction content and grain size of lacustrine sediments in Sikouzi (Fig. 6c) in southwestern CLP, a sequence that spans the last 20.1 Ma. They found low content and smaller grain size of the 10–70 μm fraction, suggesting weak EAWM intensity from 20.1 to 12.0 Ma.

Desertification

As described above, the deposition of loess started as early as 24 Ma in the Junggar Basin and 25 Ma in the western CLP. At Aertashi, in the southwestern part of the Tarim Basin, pale yellowish loess-like siltstone appears at approximately the Oligocene/Miocene boundary (OMB) (Zheng et al. 2015). Thus, desertification over a wide area of the middle latitudes of the Asian interior seems to have commenced at or slightly before the OMB. The "Miocene" loess in the western CLP was probably derived from the Gobi-Altai area (Chen and Li 2013), but its deposition was restricted to the western CLP until ca. 12 Ma. In the Tarim Basin, pale yellowish loess-like siltstone continued to accumulate until at least ca. 10 Ma after when record of the Xiyu Conglomerate cannot be found.

Post-middle Miocene

EASM

Qiang et al. (2011) described the temporal development of wet conditions in the western CLP between 16 and 14 Ma, based on an increase in the magnetic susceptibility of loess. A similar development of wet conditions was documented in the Jungger Basin between 17.5 and 13.5 Ma (Sun et al. 2010a). It is noteworthy that these wet periods coincide with the Miocene climatic optimum (17 to 15 Ma), which was most likely induced by higher atmospheric pCO_2 (Foster et al. 2012). After ca. 14 Ma, dry conditions prevailed in the western CLP until

ca. 10 Ma (Guo et al. 2002). Based on the pollen assemblage from fluvio-lacustrine sediments in Guyuan (Fig. 6c), Jiang and Ding (2008) argued for a drastic decrease in EASM precipitation from 14.25 to 11.35 Ma.

Further intensification of the warm and wet climate in East Asia occurred during the late Miocene to early Pliocene, suggesting intensification of the EASM (e.g., An et al. 2001). In the central and eastern parts of the CLP, deposition of the Red Clay Formation started at ~11–7 Ma (Sun et al. 2010b; Xu et al. 2009). Based on geochemical and sedimentological evidence, the Red Clay Formation is considered to be of eolian loess origin, but has suffered from significant pedogenesis and/or diagenesis (Guo and Peng 2001). This implies that expansion of the dry area to the west or northwest of the CLP and/or intensification of the Siberian High during winter, which supplied dust to the CLP, occurred simultaneously with intensified precipitation in the CLP during summer. However, this dry–wet shift is diachronous with the earlier shift that occurred in northeast China (Qiang et al. 2011). The magnetic susceptibility of the Red Clay Formation, considered to be a reflection of summer precipitation, increased after ca. 4.2 Ma and reached the maximum between ca. 3.2 and 2.8 Ma. This maximum occurred at approximately the same time as the mid-Pliocene warm period (e.g., An et al. 2001; Sun et al. 2010b).

Pedogenesis weakened in the CLP after ca. 2.8 Ma, suggesting weakening of the EASM (An et al. 2001). Sun et al. (2010b) demonstrated a decrease in magnetic susceptibility, and thus EASM precipitation, with increasing orbital-scale variability that started at 2.75 Ma and continued until ca. 1.25 Ma. At this time, the amplitude of orbital-scale variability further increased alongside a trend toward slightly increased magnetic susceptibility. A further increase in magnetic susceptibility and the amplitude of orbital-scale variability occurred at ca. 0.5 Ma (see also Kukla and An 1989), implying stronger summer monsoons during interglacial maxima. Based on analytical results from a drill core retrieved from the central Tengger Desert, Li et al. (2014) reported a significant deposition of eolian dust that started at 2.6 Ma with the initial formation of the Tengger Desert at 0.9 Ma and a prevalence of eolian sand deposition similar to the present started at 0.68 Ma. Pollen and organic carbon isotope records from the CLP (An et al. 2005; Wu et al. 2007) also suggest a shift to a drier climate at ca. 0.9 Ma and deposition of "mountain loess" on the southern margin of the Tarim Basin started at ca. 0.9 Ma (Fang et al. 2002).

It should be noted that the onset of the northern hemisphere glaciation (NHG) began ca. 2.8 Ma (Raymo 1994; Ruddiman 2010). The effect of the NHG on the EASM should be removed when evaluating the impact of the HTP uplift on monsoon intensity (Lu et al. 2010). It also should be noted that the Mid-Pleistocene Transition (MPT) occurred from 1.2 to 0.7 Ma and is defined as the transition interval between a change in the dominant periodicity of climate from 41 to 100 k.y. in the absence of a substantial change in orbital forcing (Clark et al. 2006; Elderfield et al. 2012). Furthermore, an age of ca. 0.5 Ma corresponds to the Mid Brunhes event that was characterized by an increase in the interglacial atmospheric pCO_2 level (e.g., EPICA Community Members 2004).

In an oxygen and carbon isotopic study of mammal teeth from central Pakistan, Martin et al. (2011) reported significantly low $\delta^{18}O$ values during 15 to 12 Ma, which they interpreted as reflecting higher precipitation and lower temperatures. An increase in $\delta^{18}O$ of mammal tooth samples from central Pakistan occurred between 12 and 9.3 Ma, and its variability increased after that time (Martin et al. 2011). Similar $\delta^{18}O$ shifts in Siwalik paleosols are reported at 9.15 Ma (e.g., Quade et al. 1989, Quade and Cerling 1995), which is interpreted to reflect a decrease in precipitation and/or an increase in the seasonality of precipitation, consistent with the reduced weathering seen in the Arabian and South China seas (Clift et al. 2008). $\delta^{13}C$ values during 15 to 12 Ma are similar to those during the Oligocene to early Miocene, suggesting the dominance of C_3 vegetation (Martin et al. 2011). The plant record from the Nepal Siwaliks during the middle Miocene indicates tropical evergreen forests with rare moist deciduous species flourished in these regions (Prasad 1993).

EAWM

The contribution of the 10–70 μm fraction to lacustrine sediments from Sikouzi increased drastically from 13 to 12 Ma. This was followed by a decrease from 12.0 to 10.3 Ma, an increase from 10.3 to 7.8 Ma, a decrease from 7.8 to 4.3 Ma, and finally a gradual increase from 4.3 to 0.07 Ma (Jiang and Ding 2010). Intensification of the EAWM at 13 to 12 Ma agrees relatively well with the onset of deposition of the Red Clay Formation in the eastern CLP at 11 Ma (Xu et al. 2009). Even though deposition of the Red Clay Formation in the main part of the CLP only started between 8 and 7 Ma, this could have been a result of the slow uplift and erosion of the Ordos Platform before 8 Ma that caused erosion or non-deposition of eolian dust on the plateau (Xu et al. 2009).

Sun et al. (2010b) analyzed the quartz grain size of loess–paleosol and Red Clay sequences at Lingtai in the central CLP over the last 7 m.y. (Fig. 6c). They concluded that the EAWM was relatively strong and had high orbital-scale variation at 7 Ma. However, the strength and amplitude of the EAWM gradually

decreased toward 4.2 Ma, reaching minima between 4.2 and 2.75 Ma. The intensity gradually increased again toward the present with a relatively abrupt increase in amplitude at 1.25 Ma. Similar results were obtained from analysis of grain size in bulk samples and accumulation of loess from multiple sites in the CLP covering the last 7.6 Ma (Sun et al. 2008a).

Ding et al. (2000) examined spatiotemporal changes in the grain size of eolian dust in loess–paleosol and Red Clay sequences in the CLP. They found a southward decrease in the grain size for loess–paleosol sequences, implying a strong influence from northerly EAWM winds after 2.6 Ma. In contrast, there is no clear trend toward decreasing grain size for the Red Clay Formation. They suggested a significant reorganization of atmospheric circulation at 2.6 Ma, with a smaller EAWM wind influence before 2.6 Ma. In this respect, it is interesting to note that orbital-scale EASM and EAWM intensities were in phase before 3.75 Ma but out-of-phase after 2.75 Ma, with a transitional period between these times (Sun et al. 2010b). After 2.6 Ma, eolian grain size shows an increasing trend, with an abrupt increase in amplitude at ca. 1.2 Ma (Sun et al. 2008a, Sun et al. 2010b).

Desertification

The occurrence of aeolian deposits provides direct evidence for the presence of deserts, and their provenance provides information on the location and extent of deserts. Deposition of the Red Clay Formation expanded into the eastern CLP at 11 Ma (Xu et al. 2009), with the Qilian Mountains as the dominant source region (Chen and Li 2013), suggesting that a desert distribution comparable to that of the present was established by ca. 11 Ma. Chen and Li (2013) also reported that the relative contribution from the Gobi Altay Mountains recovers rapidly toward early Miocene levels at ca. 1.2 Ma. The reason for this is not certain, but considering that the loess–paleosol sequence in the CLP was derived primarily from the Tennger Desert during interglacials and from the Monglian Gobi Desert during glacials (Sun et al. 2008a), intensification of EAWM wind system during glacials after 1.2 Ma is one possible cause for this change. According to a new chronology from Zheng et al. (2015), there is no sedimentary record preserved between 10 and 1 Ma in the southwestern Tarim Basin, and deposition of "Mountain Loess" started from ca. 1 Ma on the southern margin of the Tarim Basin (Fang et al. 2002).

Summary

In summary, there is evidence for a summer monsoon during the Eocene, especially in East Asia. This was probably driven by higher atmospheric pCO_2, although the latitudinal zonal distribution of climate was maintained (Huber and Goldner 2012; Zhang et al. 2012b; Licht et al. 2014). Disruption of this pattern and development of a warm and wet climate in eastern China occurred around the Oligocene/Miocene boundary at ca. 23 Ma (Sun and Wang 2005; Guo et al. 2008). After that time, a temporal increase in EASM intensity occurred during 16–14 Ma and 4.2–2.8 Ma in the CLP (e.g., Guo et al. 2002; Sun et al. 2010a) that approximately coincide with periods of temporal global warming (Raymo et al. 1996; Foster et al. 2012). Since ca. 2.8 Ma, the EASM appeared to have weakened alongside an increase in orbital-scale variability (An et al. 2001) that coincided with the onset of northern hemisphere glaciation.

It seems that the EAWM was active since as long ago as 20 Ma, but was likely very weak until 13–12 Ma when it began to intensify. The second phase of EAWM intensification occurred at ca. 2.6 Ma alongside the reorganization of atmospheric circulation. The third phase of intensification occurred at 1.2 Ma, when EAWM intensity further increased during glacial periods (Sun et al. 2010a). Superimposed on these stepwise intensifications of the EAWM are short-lived decreases in its intensity during ca. 12 to 10 and 5 to 3 Ma; the latter roughly corresponds to the time of mid-Pliocene warmth (Raymo et al. 1996).

There is increasing evidence for extensive desertification in inland Asia that began near the Oligocene/Miocene boundary at ca. 23 Ma (e.g., Guo et al. 2002; Sun et al. 2010b; Zheng et al. 2015). The second phase of desertification probably occurred at ca. 11 Ma when the Red Clay Formation began to be deposited in the eastern CLP (Xu et al. 2009). Further expansion of the dry area might have occurred at ca. 2.6 Ma and ca. 1.2 Ma (Sun et al. 2010a; Chen and Li 2013), which occurred at about the same time as the NHG and MPT, respectively.

Testing the linkage between the HTP uplift and Asian monsoon evolution

Three major phases of the HTP uplift are described in this review (see the third section and Fig. 7). The first pulse of the uplift in the south and central TP raised the area to close to its present height during the late Eocene (ca. 40 Ma). According to climate model simulations, the uplift of the southern TP would have enhanced the ISM and intensified the Somali Jet (Boos and Kuang 2010; Zhang et al. 2012b; Chen et al. 2014). Unfortunately, no sedimentary sequences are available that record the late Eocene history of ISM. Deformation and exhumation started at the northern edge of the TP and Pamir soon after the collision and accelerated at ca. 36–35 Ma, although we have no evidence that the northern TP was raised to the present level at this time.

In the Xining Basin in the northeastern TP, aridification started at ca. 36.6 Ma and was immediately followed

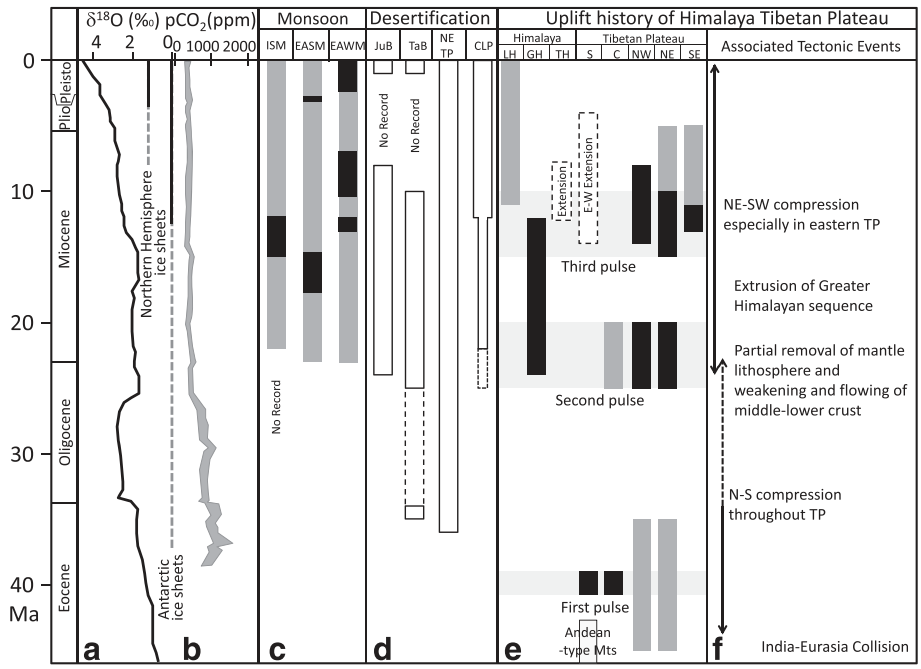

Fig. 7 Evolution of Asian monsoons, desertification, HTP uplift, and their relation with global changes during Cenozoic. Temporal changes of **a** $\delta^{18}O$ of benthic foraminifera (modified from Zachos et al. 2001) and **b** pCO_2 (modified from Zhang et al. 2013) are compared with temporal evolution of **c** Asian monsoons, **d** desertification, **e** HTP uplift, and **f** associated tectonic events. In **c** and **e**, *gray bars* represent weak phases and *black bars* represent strong phases. In **d**, JuB and TaB indicate Jungger Basin and Tarim Basin, respectively

by cooling at 36.4 Ma (Hoorn et al. 2012). This cooling preceded the EOB and Antarctic ice sheet formation by more than 2 m.y. (Coxall et al. 2005). Considering that strontium isotope ratios of seawater recorded in foraminifera started to increase at ca. 40 Ma (Richter et al. 1992), it is possible that the uplift of the northern TP and the subsequent increase in erosion started enhancing chemical weathering at ca. 40 Ma. This weathering could, in turn, have caused the drawdown of atmospheric pCO_2 (Pagani et al. 2005, 2011) and consequent cooling and aridification at ca. 36.5 Ma. This cooling and aridification would have occurred at least in Central East Asia, but was more likely hemispheric in its extent. The increase in oceanic lithium isotope ratios is also consistent with increasing silicate chemical weathering at ca. 35 Ma (Misra and Froelich 2012). Furthermore, it is likely that global cooling, together with the opening of the Drake Passage, led to the formation of Antarctic ice sheets at the EOB (DeConto and Pollard 2003) that further enhanced global cooling and aridification.

The second pulse of the HTP uplift occurred between 25 and 20 Ma in the northeastern, northwestern, and central TP and also in the Pamir (Sobel and Dumitru 1997; George et al. 2001; Wang et al. 2008; Lease et al. 2011; Amidon and Hynek 2010; Zhang et al. 2011; Xiao et al. 2012). This uplift pulse was extensive and associated with a change in deformation mode, which is interpreted to have been related to the partial removal of lithospheric mantle under northern Tibet and subsequent weakening of the middle to lower crust (Clark and Royden 2000; Royden et al. 2008; Yuan et al. 2013). Initiation of south-dipping intracontinental subduction occurred between North Pamir and the Tien Shan. This process may have been triggered by a break-off of the western end of the north-dipping Indian slab (Sobel et al. 2013) and subsequent weakening and outward flowing of the middle to lower crust (Clark and Royden 2000; Royden et al. 2008; Yuan et al. 2013), allowing the TP to reach the limiting (present-day) elevation.

According to climatic simulations of partial or phased uplift of the HTP, the uplift of the northern TP enhanced summer precipitation in northern East Asia and the southern and eastern TP (Zhang et al. 2012b; Tang et al. 2012; Chen et al. 2014), reduced precipitation in central Asia (Zhang et al. 2012a), and strengthened ISM precipitation in northern India (Boos and Kuang 2010; Zhang et al. 2012a; Chen et al. 2014). Whole uplift of the TP may also have reduced precipitation over the Somali Jet area, northern India, and southeastern Asia (Abe et al. 2003; Chen et al. 2014), while intensifying the Siberian–Mongolian high and resulting in the gradual northward movement of its center during the winter (Liu and Yin 2002).

These predictions are generally consistent with recently published paleoclimatic data described in the fourth section. In particular, a latitudinally zonal climate pattern during the Paleogene changed to a Neogene pattern. This pattern was characterized by arid zones restricted to the northwest of China and the development of a warm and wet climate in eastern China at the OMB (ca. 23 Ma), suggesting intensification of the EASM (Sun et al. 2006; Guo et al. 2008). There is also evidence of desertification in central Asia around the OMB or slightly earlier (Guo et al. 2002; Sun et al. 2010a; Qiang et al. 2011) and emergence of the EAWM by ca. 20 Ma at the latest (Jiang and Ding 2010). Although the partial HTP uplift models predict a reduction in ISM precipitation in northern India in response to the uplift of the northern TP, $\delta^{18}O$ of mammal teeth from central Pakistan and erosion rates in the Himalaya (Clift et al. 2008) suggest a shift to wetter conditions from 22 to 15 Ma (Martin et al. 2011). This contradiction can be explained by the effect of the concurrent uplift of the main part of Tibet that overwhelmed the effect of the northern TP uplift on rainfall in South Asia. However, a complete understanding of this contradiction requires additional tectonic and paleoclimatic evidence. There is some evidence of decreasing atmospheric pCO_2 around 26 Ma (Pagani et al. 2005, 2011) that may explain desertification in inland Asia. However, simultaneous development of a warm and wet climate in East Asia and central Pakistan cannot be explained by the decrease in pCO_2.

The third pulse of the HTP uplift occurred at ca. 15 to 10 Ma when the TP expanded toward the northeast and the southeast (Clark et al. 2005). This event is possibly related to the cessation of rapid Greater Himalayan exhumation. It is also suggested that the LH sequence was uplifted beginning at ca. 11 Ma (Caddick et al. 2007). As described in the second section, climate simulations predict that the uplift of the northern TP would enhance the northwest penetration of the EASM front, the desertification of inland Asia, and strengthening of the EAWM. Models also predict a decrease in ISM precipitation in northern India (Tang et al. 2012). There is some evidence that the EAWM strengthened at ca. 13 to 12 Ma (Jiang and Ding 2010) and that the deposition of loess (Red Clay formation) expanded into the eastern CLP by 11 Ma (Xu et al. 2009). The $\delta^{18}O$ of mammal teeth also provide evidence for a decrease in precipitation in central Pakistan between 12 and 9.3 Ma (Martin et al. 2011). These observations are consistent with climatic simulation predications. However, there is no clear evidence that the EASM intensified during this period. Rather, there is evidence of a drastic decrease in EASM precipitation from 14.25 to 11.35 Ma (Jiang and Ding 2008), which contradicts modeling predictions.

It should be noted that the time between 14.25 and 11.35 Ma coincides exactly with an interval of global cooling, most likely caused by the decrease in pCO_2 (Tripati et al. 2009) and consequent expansion of the Antarctic ice sheet (Holbourn et al. 2013). It is possible that intensification of the EASM caused by the uplift of northern TP was canceled out by global cooling. Alternatively, it is possible that desertification of inland Asia, intensification of the EAWM, and the reduction of ISM precipitation in northern India were caused by the decrease in pCO_2 and subsequent global cooling rather than by the uplift of the northern TP. More detailed examination of the timing and temporal sequence of the uplift of the northern TP, along with climatic changes such as intensification of the EASM and EAWM, desertification of inland Asia, reduction of ISM precipitation in northern India, and the pCO_2 decrease/global cooling is necessary in the future.

There is evidence that tectonic activity in the northern TP has not been as intensive since ca. 10 Ma as previously believed. For example, the period from ca. 3.6 to 2.6 Ma is thought to have been characterized by intensification of both the EASM and EAWM on the CLP in response to the uplift of the northern TP (e.g., An et al. 2001). However, detailed examination of the magnetic susceptibility of the Red Clay Formation suggests the opposite result. Namely, the intensity of the EASM increased from 4.2 Ma and reached a maximum at ca. 3 Ma, whereas EAWM intensity was weakest and its amplitude was at a minimum between 4.2 and 2.75 Ma (Sun et al. 2010a). This inverse trend between the intensities of the EASM and EAWM between 4.2 and 2.8 Ma is opposite to model predictions that show simultaneous intensification of the EASM and EAWM in response to the uplift of the northern TP. The data are instead consistent with a scenario where an increase in atmospheric pCO_2 affects the intensities of the EASM and EAWM. In fact, the interval between 4.2 and 2.8 Ma is approximately coincident with the Mid-Pliocene warm period from ca. 4.5 to 3.0 Ma (Wara et al. 2005) or 3.0 to 3.3 Ma (Dowsett and Robinson 2009; Haywood et al. 2005) and relatively high pCO_2 at ca. 3.3 Ma (Tripati et al. 2009). Thus, the impact of the HTP uplift on the strength of the EASM and EAWM seems minor compared with that of pCO_2 changes. However, it is still an open question whether the HTP uplift controlled the atmospheric pCO_2 level that in turn affected the evolution of both the EASM and EAWM.

Conclusions

The hypothesis that the uplift of the HTP intensified the Asian Monsoon has attracted attention from the geoscience community for more than 40 years. Yet it is still

not proven that plateau uplift intensified the monsoon because we have insufficient knowledge of both the tectonic evolution of the HTP and the paleoclimatic evolution of the Asian monsoon during the Cenozoic. In addition, climate models are not sophisticated enough to incorporate detailed topography and other boundary conditions at each stage of the uplift. However, this situation is changing rapidly with drastic increase in new data with new and sophisticated analytical techniques, as well new simulation results with more advanced high-resolution models become available. In this review, we summarized recent progress in climate model simulations that examine the impact of the HTP uplift on the evolution of the Asian monsoon, the tectonic history of the HTP uplift, and paleoclimatic evolution of the Asian monsoon during the Cenozoic.

Results of recent climate model simulations demonstrate that only the Himalaya or the southern TP are necessary to intensify the ISM, whereas the uplift of the northern TP is critical for intensification of the EASM and EAWM. The uplift of the northern TP also reduces ISM precipitation in northern India, strengthens the western North Pacific subtropical high, and reduces precipitation in central Asia. The uplift of the TP intensifies the EAWM through strengthening of the Siberian High, but the effect of stepwise uplift of the TP on the EAWM is not well explored. The effect of the Paratethys on the Asian monsoon could also be significant, but the timing of this effect is restricted to the Eocene, since this water body largely disappeared during the Oligocene. The effect of pCO_2 on the intensity of the Asian monsoon is potentially significant and should be taken into account. PCO_2 has opposing impacts on summer and winter monsoons, and its effects also contrast with the tectonically driven impact.

Three major phases of the HTP uplift are recognized. The first pulse involves the uplift of the southern and central TP at ca. 40–35 Ma, which was probably caused by the collision of the Indian subcontinent with Eurasia at ca. 50–40 Ma. The second pulse is the uplift of the northern TP at ca. 25–20 Ma, which was characterized by a change in deformation mode, probably linked to the partial removal of lithospheric mantle under the northern TP and subsequent thickening of the middle to lower crust. The Greater Himalayan sequence was exhumed and thrusted over the Lesser Himalaya sequence at that time. The third pulse is the uplift of the northeastern and eastern TP starting at ca.15–10 Ma, which may have been triggered by the expansion of the partial melting zone under the TP and propagation of the compressive front into Eurasia. Since ca. 10 Ma, the uplift has continued in the northeastern part of the TP and in the frontal Himalaya, where the progressive southward shift of the uplift continues.

The effect of the uplift of different parts of the HTP on climate was explored based on a comparison of climate model simulation results with paleoclimate records. The following changes in the Asian monsoon in various parts of Asia are predicted to be caused by differential uplift:(i) the uplift of the southern and central TP at 40–35 Ma should have intensified the ISM and the Somali Jet; (ii) the uplift of the northern TP at 25–20 Ma is predicted to have caused intensification of the EASM and EAWM, as well as the desertification of Central Asia; and (iii) the uplift of the northeastern and eastern TP at 15–10 Ma should have further intensified both the EASM and EAWM.

These predictions are tested by comparing the results with paleoclimatic data spanning critical time intervals. There are not enough paleoclimatic data to specify whether the ISM and Somali Jet intensified in association with the uplift of the southern and central TP at 40–35 Ma. However, it is possible that the uplift of the southern and central TP enhanced erosion and weathering of the HTP. This weathering may have in turn resulted in a draw down of atmospheric CO_2 and global cooling, along with expansion the Antarctic ice sheets and a reduction in EASM intensity. There is strong evidence that, beginning at 25–20 Ma, the EASM and EAWM intensified and desertification in inland Asia was enhanced in association with the uplift of the northern TP. The impact of the uplift of the northeastern and eastern TP on Asian monsoon strength at 15–10 Ma is difficult to evaluate because this interval is also a time of global cooling and Antarctic glaciation that might also have confounded Asian monsoon intensity.

In conclusion, the uplift of the northern TP at ca. 25 to 20 Ma probably triggered the establishment of the EASM and desertification of inland Asia. However, as with the other two uplift phases that affected the HTP at ca. 40–35 Ma and 15–10 Ma, paleoclimatic data are still insufficient to clearly demonstrate this linkage. It is clear that other boundary conditions, especially the atmospheric pCO_2 level, also exert an influence on Asian monsoons. Thus, we must differentiate such effects from the effect of the HTP uplift to properly evaluate its impact. However, it is important to note that the uplift and subsequent erosion of the HTP may also affect the atmospheric pCO_2 level through chemical weathering. The intensity of chemical weathering is also influenced by summer monsoon precipitation. Tectonics and climate linkages are not a one-way process, and many feedback loops are still waiting to be discovered.

Abbreviations
AGCM: atmospheric GCM; CGCM: atmosphere–ocean coupled GCM; CLP: Chinese Loess Plateau; EAM: East Asian monsoon; EASM: East Asian summer monsoon; EAWM: East Asian winter monsoon; EOB: Eocene–Oligocene boundary; EOT: Eocene–Oligocene Transition; GCM: general circulation models; GCT: Great Counter Thrust; HHC: Higher Himalayan Crystalline; HTP: Himalaya and Tibetan Plateau; IODP: Integrated Ocean Drilling Program; ISM: Indian summer monsoon; LH: Lesser Himalaya; MBT: Main Boundary Thrust; MCT: Main Central Thrust; MFT: Main Frontal Thrust; MPT: mid-Pleistocene transition; NHG: northern hemisphere glaciation; ODP: Ocean Drilling Program; OMB: Oligocene–Miocene boundary; SST: sea surface temperature; STDS: Southern Tibetan Detachment System; TP: Tibetan Plateau; WJ: westerly jet.

Competing interests
The authors declare that they have no competing interests.

Authors' contributions
RT wrote the draft manuscript. HZ and PC read the draft and corrected and modified specific sections based on their expertise. All authors read and approved the final manuscript.

Authors' information
RT is a professor in the Department of Earth and Planetary Science, Graduate School of Science, University of Tokyo. He is an expert in sedimentology, paleoceanography, and paleoclimatology. HZ is a professor in the School of Geography Science, Nanjing Normal University. He is an expert in sedimentology and tectonic geology and has a wide knowledge of the geology of China. PC is a professor in the Department of Geology and Geophysics, Louisiana State University. He is an expert in sedimentology, seismic geology, and tectonics of the Himalaya and Tibet. RT was a leader of IGCP-476 (2003–2007; Monsoon Evolution and Tectonics–Climate Linkage in Asia) and HZ and PC were co-leaders. HZ was a leader of IGCP-581 (2009–2014; Evolution of Asian River Systems) and RT and PC were co-leaders. This review is a summary of the results of these two projects, together with other new knowledge and findings.

Acknowledgements
We thank Professors Iryu and Kawahata, and other editorial board and editorial office members of PEPS for their support and encouragement. We also thank two anonymous reviewers and Dr. Youbin Sun for critical comments and constructive suggestions. Thanks also go to Mrs. Ashino for collecting and editing the references cited in this paper.

Author details
[1]Department of Earth and Planetary Science, Graduate School of Science, The University of Tokyo, 7-3-1 Hongo, Bunkyo-ku, Tokyo 113-0033, Japan. [2]School of Geography Science, Nanjing Normal University, 1 Wenyuan Road, Xianlin University Town, Nanjing, China. [3]Department of Geology and Geophysics, E235 Howe-Russell-Kniffen Geoscience Complex, Louisiana State University, Baton Rouge, LA 70803, USA.

Received: 8 June 2015 Accepted: 18 January 2016
Published online: 09 February 2016

References
Abe M, Kitoh A, Yasunari T (2003) An evolution of the Asian summer monsoon associated with mountain uplift—simulation with the MRI atmosphere–ocean coupled GCM. J Meteorol Soc Jpn 81(5):909–933
Abe M, Yasunari T, Kitoh A (2004) Effects of large-scale orography on the coupled atmosphere–ocean system in the tropical Indian and Pacific Oceans in Boreal summer. J Meteorol Soc Jpn 82(2):745–759
Abels HA, Dupont-Nivet G, Xiao G, Bosboom R, Krijgsman W (2011) Step-wise change of Asian interior climate preceding the Eocene–Oligocene Transition (EOT). Palaeogeogr Palaeoclimatol Palaeoecol 299(3–4):399–412. doi:10.1016/j.palaeo.2010.11.028
Amidon WH, Hynek SA (2010) Exhumational history of the north central Pamir. Tectonics 29(5):1–13. doi:10.1029/2009tc002589
An Z, Kutzbach JE, Prell WL, Porter SC (2001) Evolution of Asian monsoons and phased uplift of the Himalaya-Tibetan plateau since late Miocene times. Nature 411:62–66
An Z, Huang Y, Liu W, Guo Z, Steven C, Li L et al (2005) Multiple expansions of C_4 plant biomass in East Asia since 7 Ma coupled with strengthened monsoon circulation. Geology 33(9):705–708. doi:10.1130/g21423.1
Antonie PO, Downing KD, Crochet JY, Duranthon F, Flynn L, Marivaux L et al (2010) A revision of *Aceratherium blanfordi* Lydekker, 1884 (Mammalia: Rhinocerotidae) from the Early Miocene of Pakistan: postcranials as a key. Zool J Linn Soc 160:139–194. doi:10.1111/j.1096-3642.2009.00597
Armstrong HA, Allen MB (2010) Shifts in the intertropical convergence zone, Himalayan exhumation, and late Cenozoic climate. Geology 39(1):11–14. doi:10.1130/g31005.1
Bershaw J, Garzione CN, Schoenbohm L, Gehrels G, Tao L (2012) Cenozoic evolution of the Pamir plateau based on stratigraphy, zircon provenance, and stable isotopes of foreland basin sediments at Oytag (Wuyitake) in the Tarim Basin (west China). J Asian Earth Sci 44:136–148. doi:10.1016/j.jseaes.2011.04.020
Blisniuk PM, Hacker BR, Glodny J, Ratschbacher L, Bi S, Wu Z et al (2001) Normal faulting in central Tibet since at least 13.5 Myr ago. Nature 412:628–632
Boos WR, Kuang Z (2010) Dominant control of the South Asian monsoon by orographic insulation versus plateau heating. Nature 463(7278):218–222. doi:10.1038/nature08707
Boos WR, Kuang Z (2013) Sensitivity of the South Asian monsoon to elevated and non-elevated heating. Sci Rep 3:1192. doi:10.1038/srep01192
Broccoli AJ, Manabe S (1992) The effects of orography on midlatitude Norhern Hemisphere dry climates. J Clim 5:1181–1201
Caddick M, Bickle M, Harris N, Holland T, Horstwood M, Parrish R et al (2007) Burial and exhumation history of a Lesser Himalayan schist: recording the formation of an inverted metamorphic sequence in NW India. Earth Planet Sci Lett 264(3–4):375–390. doi:10.1016/j.epsl.2007.09.011
Catlos EJ, Dubey CS, Harrison TM, Edwards MA (2004) Late Miocene movement within the Himalayan Main Central Thrust shear zone, Sikkim, north-east India. Geology 22:207–226. doi:10.1111/j.1525-1314.2004.00509
Caves JK, Winnick MJ, Graham SA, Sjostrom DJ, Mulch A, Chamberlain CP (2015) Role of the westerlies in Central Asia climate over Cenozoic. Earth Planet Sci Lett 428:33–43. doi:10.1016/j.epsl.2015.07.023
Chakraborty ANRS, Srinivasan J (2006) Theoretical aspects of the onset of Indian summer monsoon from perturbed orography simulations in a GCM. Ann Geophys 24:2075–2089
Chang CP, Wang Z, Hendon H (2006) The Asian Winter Monsoon. Praxis. Springer, Berlin Heideelberg, Berlin
Charney JG (1975) Dynamics of deserts and drought in the Sahel. Quart J R Meteor Soc 101:193–202
Chen Z, Li G (2013) Evolving sources of eolian detritus on the Chinese Loess Plateau since early Miocene: Tectonic and climatic controls. Earth Planet Sci Lett 371–372:220–225. doi:10.1016/j.epsl.2013.03.044
Chen FH, Cheng B, Zhao Y, Zhu Y, Madsen DB (2006) Holocene environmental change inferred from a high-resolution pollen record, Lake Zhuyeze, arid China. The Holocene 16(5):675–684
Chen GS, Liu Z, Kutzbach JE (2014) Reexamining the barrier effect of the Tibetan Plateau on the South Asian summer monsoon. Clim Past 10(3):1269–1275. doi:10.5194/cp-10-1269-2014
Christensen JH, Krishna K, Aldrian KK, An S-I E, Cavalcanti IFA, de Castro M et al (2013) Climate Phenomena and their Relevance for Future Regional Climate Change. In: Stocker TF, Qin D, Plattner GK, Tignor M, Allen SK, Boschung J, Nauels A, Xia Y, Bex V, Midgley PM (eds) Climate Change 2013: The Physical Science Basis. Contribution of Working Group I to the Fifth Assessment Report of the Intergovernmental Panel on Climate Change Cambridge University Press, Cambridge and New York
Clark MK (2012) Continental collision slowing due to viscous mantle lithosphere rather than topography. Nature 483(7387):74–77. doi:10.1038/nature10848
Clark MK, Royden LH (2000) Topographic ooze: building the eastern margin of Tibet by lower crustal flow. Geology 28(8):703–706
Clark MK, House MA, Royden LH, Whipple KX, Burchfiel BC, Zhang X et al (2005) Late Cenozoic uplift of southeastern Tibet. Geology 33(6):525. doi:10.1130/g21265.1
Clark PU, Archer D, Pollard D, Blum JD, Rial JA, Brovkin V et al (2006) The middle Pleistocene transition: characteristics, mechanisms, and implications for long-term changes in atmospheric pCO_2. Quat Sci Rev 25(23–24):3150–3184. doi:10.1016/j.quascirev.2006.07.008

Clark MK, Farley KA, Zheng D, Wang Z, Duvall AR (2010) Early Cenozoic faulting of the northern Tibetan Plateau margin from apatite (U–Th)/He ages. Earth Planet Sci Lett 296(1–2):78–88. doi:10.1016/j.epsl.2010.04.05

Clift PD, Carter A, Krol M, Kirby E (2002) Constraints of India Eurasia collision in the Arabian Sea region taken from the Indus Group, Ladakh Himalaya, India. In: Clift PD, Kroon D, Gaedicke C, Craig J (eds) The tectonic and climatic evolution of the Arabian Sea region. J Geol Soc Special Publication., pp 97–116

Clift PD, Hodges KV, Heslop D, Hannigan R, Van Long H, Calves G (2008) Correlation of Himalayan exhumation rates and Asian monsoon intensity. Nat Geosci 1(12):875–880. doi:10.1038/ngeo351

Clift PD, Wan S, Blusztajn J (2014) Reconstruction chemical weathering, physical erosion and monsoon intensity since 25 Ma in the northern south china Sea: a review of competing proxies. Earth-Sci Rev 130:86–102. doi:10.1016/j.earscirev.2014.01.002

Coxall HK, Wilson PA, Palike H, Lear CH, Backman J (2005) Rapid stepwise onset of Antarctic glaciation and deeper calcite compensation in the Pacific Ocean. Nature 433(7021):53–57. doi:10.1038/nature03135

Craddock WH, Kirby E, Harkins NW, Zhang H, Shi X, Liu J (2010) Rapid fluvial incision along the yellow river during headward basin integration. Nat Geosci 3(3):209–213. doi:10.1038/ngeo777

Dai J, Zhao X, Wang C, Zhu L, Li Y, Finn D (2012) The vast proto-Tibetan plateau: New constraints from paleogene Hoh Xil basin. Gondwana Res 22(2):434–446. doi:10.1016/j.gr.2011.08.019

De Franceschi D, Hoorn C, Antoine PO, Cheema IU, Flynn LJ, Lindsay EH et al (2008) Floral data from the mid-Cenozoic of central Pakistan. Rev Palaeobot Palynology 150(1–4):115–129. doi:10.1016/j.revpalbo.2008.01.011

Decelles PG, Robinson DM, Quade J, Ojha TP, Garzione CN, Copeland P et al (2001) Stratigraphy, structure, and tectonic evolution of the Himalayan fold-thrust belt in western Nepal. Tectonics 20(4):487–509. doi:10.1029/2000tc001226

Deconto RM, Pollard D (2003) Rapid Cenozoic glaciation of Antarctica induced by declining atmospheric CO_2. Nature 421:245–249

Deeken A, Thiede RC, Sobel ER, Hourigan JK, Strecker MR (2011) Exhumational variability within the Himalaya of northwest India. Earth Planet Sci Lett 305(1–2):103–114. doi:10.1016/j.epsl.2011.02.045

Ding ZL, Rutter NW, Sun JM, Yang SL, Liu TS (2000) Re-arrangement of atmospheric circulation at about 2.6 Ma over northern China: evidence from grain size records of loess-palaeosol and red clay sequences. Quat Sci Rev 19:547–558

Ding L, Xu Q, Yue Y, Wang H, Cai F, Li S (2014) The Andean-type Gangdese Mountains: Paleoelevation record from the Paleocene-Eocene Linzhou Basin. Earth Planet Sci Lett 392:250–264. doi:10.1016/j.epsl.2014.01.045

Dowsett HJ, Robinson MM (2009) Mid-Pliocene equatorial Pacific sea surface temperature reconstruction: a multi-proxy perspective. Philos Trans A Math Phys Eng Sci 367(1886):109–125. doi:10.1098/rsta.2008.0206

Dupont-Nivet G, Krijgsman W, Langereis CG, Abels HA, Dai S, Fang X (2007) Tibetan plateau aridification linked to global cooling at the Eocene-Oligocene transition. Nature 445(7128):635–638. doi:10.1038/nature05516

Dupont-Nivet G, Hoorn C, Konert M (2008) Tibetan uplift prior to the Eocene-Oligocene climate transition: evidence from pollen analysis of the Xining basin. Geology 36(12):987. doi:10.1130/g25063a.1

Duvall AR, Clark MK, Kirby E, Farley KA, Craddock WH, Li C et al (2013) Low-temperature thermochronometry along the Kunlun and haiyuan faults, NE Tibetan plateau: evidence for kinematic change during late-stage orogenesis. Tectonics 32(5):1190–1211. doi:10.1002/tect.20072

Edwards MA, Harrison TM (1997) When did the roof collapse? Late Miocene north–south extension in the high Himalaya revealed by Th-Pb monazite dating of the Khula Kangri granite. Geology 25(6):543–546

Elderfield H, Ferretti P, Greaves M, Crowhurst S, Mcave IN, Hodell D et al (2012) Evolution of ocean temperature and ice volume through the Mid-Pleistocene climate transition. Science 337:704–709. doi:10.1126/science.1221294

England P, Searle M (1986) The cretaceous-tertiary deformation of the Lhasa block and its implications for crustal thickening in Tibet. Tectonics 5(1):1–14

EPICA community members (2004) Eight glacial cycles from an Antarctic ice core. Nature 429:623–628

Fang X, Lu L, Yang S, Li J, An Z, Jiang P et al (2002) Loess in Kunlun Mountains and its implications on desert development and Tibetan Plateau uplift in west China. Sci China Series D: Earth Sci 45(4):289–299

Foster GL, Lear CH, Rae JWB (2012) The evolution of pCO_2, ice volume and climate during the middle Miocene. Earth Planet Sci Lett 341–344:243–254. doi:10.1016/j.epsl.2012.06.007

France-Lannord C, Derry LA (1997) Organic carbon burial forcing of the carbon cycle from Himalayan erosion. Nature 390:65–67

Gebelin A, Mulch A, Teyssier C, Jessup MJ, Law RD, Brunel M (2013) The Miocene elevation of mount Everest. Geology 41(7):799–802. doi:10.1130/G34331.1

George AD, Marshallsea SJ, Wyrowoll KH, Jie C, Yanchou L (2001) Miocene cooling in the northern Qilian Shan, northeastern margin of the Tibetan Plateau, revealed by apatite fission-track and vitrinite-reflectance analysis. Geology 29(10):939–942

Godin L, Grujic D, Law RD, Searle MP (2006) Channel flow, ductile extrusion and exhumation in continental collision zones: an introduction. J Geol Soc Special Publications 268:1–23

Graham SA, Chamberlain CP, Yue Y, Ritts BD, Hanson AD, Horton TW, Waldbauer JR, Poage MA, Feng X (2005) Stable isotope records of Cenozoic climate and topography, Tibetan plateau and Tarim basin. Am J Sci 305:101–118

Guo ZT, Peng SZ (2001) Origin of the Miocene-Pliocene Red-Earth Formation at Xifeng in Northern China and implications for paleoenvironments. Palaeogeogr Palaeoclimatol Palaeoecol 170:11–26

Guo ZT, Ruddiman WF, Hao QZ, Peng SZ (2002) Onset of Asian desertification by 22Myr ago inferred from loess deposits in China. Nature 416:159–163

Guo ZT, Peng SZ, Zhang ZS (2008) A major reorganization of Asian climate by the early Miocene. Clim Past 4:153–174

Hahn DG, Manabe S (1975) The role of mountains in the south Asian monsoon circulation. J Atmos Sci 32:1515–1541

Harris N (2006) The elevation history of the Tibetan Plateau and its implications for the Asian monsoon. Palaeogeogr Palaeoclimatol Palaeoecol 241(1):4–15. doi:10.1016/j.palaeo.2006.07.009

Harris N (2007) Channel flow and the Himalayan–Tibetan orogen: a critical review. J Geol Soc 164:511–523

Haywood AM, Dekens P, Ravelo AC, Williams M (2005) Warmer tropics during the mid-Pliocene? Evidence from alkenone paleothermometry and a fully coupled ocean–atmosphere GCM. Geochem Geophys Geosyst 6(3):1–20. doi:10.1029/2004gc000799

Hetzel R, Dunkl I, Haider V, Strobl M, Von Eynatten H, Ding L et al (2011) Peneplain formation in southern Tibet predates the India-Asia collision and plateau uplift. Geology 39(10):983–986. doi:10.1130/g32069.1

Hodges K (2006) Climate and the evolution of mountains. Sci Am 295(2):72–79

Hoke GD, Liu-Zeng J, Hren MT, Wissink GK, Garzione CN (2014) Stable isotopes reveal high southeast Tibetan Plateau margin since the Paleogene. Earth Planet Sci Lett 394:270–278. doi:10.1016/j.epsl.2014.03.007

Holbourn A, Kuhnt W, Clemens S, Prell W, Andersen N (2013) Middle to late Miocene stepwise climate cooling: evidence from a high-resolution deep water isotope curve spanning 8 million years. Paleoceanography 28:688–699. doi:10.1002/2013PA002538

Hoorn C, Straathof J, Abels HA, Xu Y, Utescher T, Dupont-Nivet G (2012) A late Eocene palynological record of climate change and Tibetan Plateau uplift (Xining Basin, China). Palaeogeogr Palaeoclimatol Palaeoecol 344–345:16–38. doi:10.1016/j.palaeo.2012.05.011

Hori ME, Ueda H (2006) Impact of global warming on the East Asian winter monsoon as revealed by nine coupled atmosphere–ocean GCMs. Geophys Res Lett 33:3. doi:10.1029/2005gl024961

Hough BG, Garzione CN, Wang Z, Lease RO, Burbank DW, Yuan D (2011) Stable isotope evidence for topographic growth and basin segmentation: Implications for the evolution of the NE Tibetan Plateau. Geol Soc Am Bull 123(1–2):168–185. doi:10.1130/b30090.1

Hren MT, Chamberlain CP, Hilley GE, Blisniuk PM, Bookhagen B (2007) Major ion chemistry of the Yarlung Tsangpo–Brahmaputra river: chemical weathering, erosion, and CO_2 consumption in the southern Tibetan plateau and eastern syntaxis of the Himalaya. Geochim Cosmochim Acta 71(12):2907–2935. doi:10.1016/j.gca.2007.03.021

Huang Y, Clemens SC, Liu W, Wang Y, Prell WL (2007) Large-scale hydrological change drove the late Miocene C_4 plant expansion in the Himalayan foreland and Arabian Peninsula. Geology 35(6):531. doi:10.1130/g23666a.1

Huber M, Goldner A (2012) Eocene monsoons. J Asian Earth Sci 44:3–23. doi:10.1016/j.jseaes.2011.09.014

Huntington KW, Blythe AE, Hodges KV (2006) Climate change and Late Pliocene acceleration of erosion in the Himalaya. Earth Planet Sci Lett 252(1–2):107–118. doi:10.1016/j.epsl.2006.09.031

Ikehara K, Itaki T (2007) Millennial-scale fluctuations in seasonal sea-ice and deep-water formation in the Japan Sea during the late Quaternary. Palaeogeogr Palaeoclimatol Palaeoecol 247(1–2):131–143. doi:10.1016/j.palaeo.2006.11.026

Itaki T, Ikehara K, Motoyama I, Hasegawa S (2004) Abrupt ventilation changes in the Japan Sea over the last 30 ky: evidence from deep-dwelling radiolarians. Palaeogeogr Palaeoclimatol Palaeoecol 208(3–4):263–278. doi:10.1016/j.palaeo.2004.03.010

Jhun JG, Lee E-J (2004) A new East Asian winter monsoon index and associated characteristics of the winter monsoon. J Clim 17:711–726

Jiang H, Ding Z (2008) A 20 Ma pollen record of East-Asian summer monsoon evolution from Guyuan, Ningxia, China. Palaeogeogr Palaeoclimatol Palaeoecol 265(1–2):30–38. doi:10.1016/j.palaeo.2008.04.016

Jiang H, Ding Z (2010) Eolian grain-size signature of the Sikouzi lacustrine sediments (Chinese Loess Plateau): Implications for Neogene evolution of the East Asian winter monsoon. Geol Soc Am Bull 122(5–6):843–854. doi:10.1130/b26583.1

Jiang H, Ji J, Gao L, Tang Z, Ding Z (2008) Cooling-driven climate change at 12–11 Ma: Multiproxy records from a long fluviolacustrine sequence at Guyuan, Ningxia, China. Palaeogeogr Palaeoclimatol Palaeoecol 265(1–2):148–158. doi:10.1016/j.palaeo.2008.05.006

Kapp P, Decelles PG, Gehrels GE, Heizler M, Ding L (2007) Geological records of the Lhasa-Qiangtang and Indo-Asian collisions in the Nima area of central Tibet. Geol Soc Am Bull 119(7–8):917–933. doi:10.1130/b26033.1

Kim DW, Byun HR (2009) Future pattern of Asian drought under global warming scenario. Theor Appl Climatol 98(1–2):137–150. doi:10.1007/s00704-008-0100-y

Kimoto M (2005) Simulated change of the East Asian circulation under global warming scenario. Geophys Res Lett 32:16. doi:10.1029/2005gl023383

Kitoh A (2002) Effects of large-scale mountains on surface climate-a coupled Ocean-Atmophere General Circulation Model study. J Meteorol Soc Jpn 80(5):1165–1181

Kitoh A (2004) Effects of mountain uplift on East Asian summer climate investigated by a coupled Atmophere-Ocean GCM. J Clim 17:783–802

Kripalani RH, Oh JH, Chaudhari HS (2007) Response of the East Asian summer monsoon to doubled atmospheric CO_2: Coupled climate model simulations and projections under IPCC AR4. Theor Appl Climatol 87(1–4):1–28. doi:10.1007/s00704-006-0238-4

Kubota Y, Kimoto K, Tada R, Oda H, Yokoyama Y, Matsuzaki H (2010) Variations of East Asian summer monsoon since the last deglaciation based on Mg/Ca and oxygen isotope of planktic foraminifera in the northern East China Sea. Paleoceanography 25:4. doi:10.1029/2009pa001891

Kubota Y, Tada R, Kimoto K (2015) Changes in East Asian summer monsoon precipitation during the Holocene deduced from a freshwater flux reconstruction of the Changjiang (Yangtze River) based on the oxygen isotope mass balance in the northern East China Sea. Clim Past 11(2):265–281. doi:10.5194/cp-11-265-2015

Kukla G, An Z (1989) Loess Stratigraphy in Central China. Palaeogeogr Palaeoclimatol Palaeoecol 72:203–225

Kutzbach JE, Guetter PJ, Ruddiman WF, Prell WL (1989) Sensitivity of climate to late Cenozoic uplift in Southern Asia and the American West: numerical experiments. J Geophys Res 94(D15):18393–18407

Lear CH (2007) Mg/Ca palaeothermometry: a new window into Cenozoic climate change. In: Williams M, Haywood AM, Gregoly FJ (eds) Deep-Time Perspectives on Climate Change: Marrying the Signal from Computer Models and Biological Proxies., pp 313–312

Lease RO, Burbank DW, Clark MK, Farley KA, Zheng D, Zhang H (2011) Middle Miocene reorganization of deformation along the northeastern Tibetan Plateau. Geology 39(4):359–362. doi:10.1130/g31356.1

Li JJ, Fang XM, Van Der Voo R, Zhu JJ, Niocill CM, Ono Y et al (1997) Magnetostratigraphic dating of river terraces: rapid and intermittent incision by the Yellow River of the northeastern margin of the Tibetan Plateasu during the Quaternary. J Geophys Res Solid Earth 102(B5):10121–10132. doi:10.1029/97JB00275

Li Z, Sun D, Chen F, Wang F, Zhang Y, Guo F et al (2014) Chronology and paleoenvironmental records of a drill core in the central Tengger Desert of China. Quat Sci Rev 85:85–98. doi:10.1016/j.quascirev.2013.12.003

Licht A, van Cappelle M, Abels HA, Ladant JB, Trabucho-Alexandre J, France-Lanord C et al (2014) Asian monsoons in a late Eocene greenhouse world. Nature 513(7519):501–506. doi:10.1038/nature13704

Liu X, Dong B (2013) Influence of the Tibetan Plateau uplift on the Asian monsoon-arid environment evolution. Chin Sci Bull 58(34):4277–4291. doi:10.1007/s11434-013-5987-8

Liu X, Yin ZY (2002) Sensitivity of East Asian monsoon climate to the uplift of the Tibetan Plateau. Palaeogeogr Palaeoclimatol Palaeoecol 183:223–245

Lu H, Wang X, Li L (2010) Aeolian sediment evidence that global cooling has driven late Cenozoic stepwise aridification in Asia. J Geol Soc Special Publications 342(1):46–65. doi:10.1144/sp342.5

Manabe S, Broccoli AJ (1990) Mountains and arid climates of middle latitudes. Science 247:192–195

Manabe S, Terpstra TB (1974) The effects of mountains on the general circulation of the atmosphere as identified by numerical experiments. J Atmos Sci 31(1):3–42

Martin C, Bentaleb I, Antoine PO (2011) Pakistan mammal tooth stable isotopes show paleoclimatic and paleoenvironmental changes since the early Oligocene. Palaeogeogr Palaeoclimatol Palaeoecol 311(1–2):19–29. doi:10.1016/j.palaeo.2011.07.010

Mcdermott JA, Whipple KX, Hodges KV, Van Soest MC (2013) Evidence for Plio-Pleistocene north–south extension at the southern margin of the Tibetan Plateau, Nyalam region. Tectonics 32(3):317–333. doi:10.1002/tect.20018

Misra S, Froelich PN (2012) Lithium isotope history of Cenozoic seawater: changes in silicate weathering and reverse weathering. Science 335(6070):818–823. doi:10.1126/science.1214697

Molnar P, Stock JM (2009) Slowing of India's convergence with Eurasia since 20 Ma and its implications for Tibetan mantle dynamics. Tectonics 28(3):1–11. doi:10.1029/2008tc002271

Molnar P, Boos WR, Battisti DS (2010) Orographic controls on climate and paleoclimate of Asia: thermal and mechanical roles for the Tibetan plateau. Annu Rev Earth Planet Sci 38(1):77–102. doi:10.1146/annurev-earth-040809-152456

Murphy MA, Saylor JE, Ding L (2009) Late Miocene topographic inversion in southwest Tibet based on integrated paleoelevation reconstructions and structural history. Earth Planet Sci Lett 282(1–4):1–9. doi:10.1016/j.epsl.2009.01.006

Nagashima K, Tada R, Matsui H, Irino T, Tani A, Toyoda S (2007) Orbital- and millennial-scale variations in Asian dust transport path to the Japan Sea. Palaeogeogr Palaeoclimatol Palaeoecol 247(1–2):144–161. doi:10.1016/j.palaeo.2006.11.027

Nagashima K, Tada R, Tani A, Sun Y, Isozaki Y, Toyoda S et al (2011) Millennial-scale oscillations of the westerly jet path during the last glacial period. J Asian Earth Sci 40(6):1214–1220. doi:10.1016/j.jseaes.2010.08.010

Nelson KD, Zhao W, Brown LD, Kuo J, Che J, Liu X et al (1996) Partially molten middle crust beneath southern Tibet: synthesis of project indepth results. Science 274:1684–1688

Ono Y, Naruse T, Ikeya M, Kohno H, Toyoda S (1998) Origin and derived courses of eolian dust quartz deposited during maine isotope stage 2 in East Asia, suggested by ESR signal. Glob Planet Change 18:129–135

Pagani M, Zachols JC, Freeman KH, Tipple B, Bohaty SM (2005) Marked decline in atmospheric carbon dioxide concentrations during the Paleogene. Science 309:600–603. doi:10.1126/science.1110063

Pagani M, Huber M, Liu Z, Bohaty SM, Henderiks J, Sijp W et al (2011) The role of carbon dioxide during the onset of Antarctic glaciation. Science 334(6060):1261–1264. doi:10.1126/science.1203909

Pearson PN, Foster GL, Wade BS (2009) Atmospheric carbon dioxide through the Eocene-Oligocene climate transition. Nature 461(7267):1110–1113. doi:10.1038/nature08447

Polissar PJ, Freeman KH, Rowley DB, Mcinerney FA, Currie BS (2009) Paleoaltimetry of the Tibetan Plateau from D/H ratios of lipid biomarkers. Earth Planet Sci Lett 287(1–2):64–76. doi:10.1016/j.epsl.2009.07.037

Prasad M (1993) Siwalik (Middle Miocene) woods from the Kalagarh area in the Himalayan foot hills and their bearing on palaeoclimate and phytogeography. Rev Palaeobot Palynology 76:49–82

Qiang XK, Li ZX, Powell CM, Zheng HB (2001) Magnetostratigraphic record of the Late Miocene onset of the East Asian monsoon, and Pliocene uplift of northern Tibet. Earth Planet Sci Lett 187:83–93

Qiang XK, An Z, Song Y, Chang H, Sun Y, Liu W et al (2011) New eolian red clay sequence on the western Chinese Loess Plateau linked to onset of Asian desertification about 25 Ma ago. Sci China Earth Sci 54(1):136–144. doi:10.1007/s11430-010-4126-5

Quade J, Cerling TE (1995) Expansion of C_4 grasses in the Late Miocene of Northern Pakistan: evidence from stable isotopes in paleosols. Palaeogeogr Palaeoclimatol Palaeoecol 115:91–116

Quade J, Cerling TE, Bowman JR (1989) Development of Asian monsoon revealed by marked ecological shift during the latest Miocene in northern Pakistan. Nature 342:163–166

Quade J, Breecker DO, Daeron M, Eiler J (2011) The paleoaltimetry of Tibet: an isotopic perspective. Am J Sci 311(2):77–115. doi:10.2475/02.2011.01

Quan C, Liu Y-S, Utescher T (2012) Eocene monsoon prevalence over China: a paleobotanical perspective. Palaeogeogr Palaeoclimatol Palaeoecol 365–366: 302–311. doi:10.1016/j.palaeo.2012.09.035

Ramstein G, Fluteau F, Besse J, Joussaume S (1997) Effect of orogeny, late motion and land-sea distribution on Eurasian climate change over the past 30 million years. Nature 386:788–795

Raymo ME (1994) The Initiation of Northern Hemisphere Glaciation. Annu Rev Earth Planet Sci 22:353–383

Raymo ME, Ruddiman WF (1992) Tectonic forcing of late Cenozoic climate. Nature 359:117–122

Raymo ME, Ruddiman WF, Froelich PN (1988) Influence of late Cenozoic mountain building on ocean geochemical cycles. Geology 16:649–653

Raymo ME, Grant B, Horowitz M, Rau GH (1996) Mid-Pliocene warmth: stronger greenhouse and stronger conveyor. Mar Micropaleontol 27:313–326

Richter FM, Rowley DB, Depaolo DJ (1992) Sr isotope evolution of seawater: the role of tectonics. Earth Planet Sci Lett 109:11–23

Ritts BD, Yue Y, Graham SA, Sobel ER, Abbink OA, Stockli D (2008) From sea level to high elevation in 15 million years: uplift history of the northern Tibetan Plateau margin in the Altun Shan. Am J Sci 308(5):657–678. doi:10.2475/05.2008.01

Rowley DB, Currie BS (2006) Palaeo-altimetry of the late Eocene to Miocene Lunpola basin, central Tibet. Nature 439(7077):677–681. doi:10.1038/nature04506

Royden LH, Burchfiel BC, Van Der Hilst RD (2008) The geological evolution of the Tibetan Plateau. Science 321(5892):1054–1058. doi:10.1126/science.1155371

Ruddiman WF (2010) A Paleoclimatic Enigma? Science 328:838–839

Ruddiman WF, Kutzbach JE (1989) Forcing of Late Cenozoic Northern Hemisphere climate by plateau uplift in Southern Asian and the American West. J Geophys Res 94(D15):18409–18427

Ruddiman WF, Prell WL (1997) Tectonic uplift and climatic change. Plenum Press, New York

Ruddiman WF, Prell WL, Raymo ME (1989) Late Cenozoic uplift in southern Asia and the American West: rationale for general circulation modeling experiments. J Geophys Res 94(D15):18379–18391

Sampe T, Xie SP (2010) Large-scale dynamics of the Meiyu-baiu rainband: environmental forcing by the Westerly jet. J Clim 23(1):113–134. doi:10.1175/2009jcli3128.1

Saylor JE, Quade J, Dettman DL, DeCelles PG, Kapp PA, Ding L (2009) The Late Miocene through present paleoelevation history of southwestern Tibet. Amer J Sci 309:1–42. doi:10.2475/01.2009.01

Schiemann R, Lüthi D, Schär C (2009) Seasonality and interannual variability of the Westerly jet in the Tibetan Plateau region. J Clim 22(11):2940–2957. doi:10.1175/2008jcli2625.1

Sobel ER, Dumitru A (1997) Thrusting and exhumation around the margins of the western Tarim basin during the India-Aisa collision. J Geophys Res 102(B3): 5043–5063

Sobel ER, Chen J, Schoenbohm LM, Thiede R, Stockli DF, Sudo M et al (2013) Oceanic-style subduction controls late Cenozoic deformation of the Northern Pamir orogen. Earth Planet Sci Lett 363:204–218. doi:10.1016/j.epsl.2012.12.009

Song ZC, Li HM, Zheng YH, Liu G (1983) In: Lu YH (ed) Miocene floristic region of China (in Chinese), in Palaeobiogeographic Provinces of China. Beijing Science Press, Beijing, pp 178–184

Sun X, Wang P (2005) How old is the Asian monsoon system?—Palaeobotanical records from China. Palaeogeogr Palaeoclimatol Palaeoecol 222(3-4):181–222. doi:10.1016/j.palaeo.2005.03.005

Sun Y, Lu H, An Z (2006) Grain size of loess, palaeosol and Red Clay deposits on the Chinese Loess Plateau: Significance for understanding pedogenic alteration and palaeomonsoon evolution. Palaeogeogr Palaeoclimatol Palaeoecol 241(1):129–138. doi:10.1016/j.palaeo.2006.06.018

Sun D, Su R, Bloemendal J, Lu H (2008a) Grain-size and accumulation rate records from Late Cenozoic aeolian sequences in northern China: implications for variations in the East Asian winter monsoon and westerly atmospheric circulation. Palaeogeogr Palaeoclimatol Palaeoecol 264(1–2):39–53. doi:10.1016/j.palaeo.2008.03.011

Sun Y, Tada R, Chen J, Liu Q, Toyoda S, Tani A et al (2008b) Tracing the provenance of fine-grained dust deposited on the central Chinese Loess Plateau. Geophys Res Lett 35:1. doi:10.1029/2007gl031672

Sun J, Ye J, Wu W, Ni X, Bi S, Zhang Z et al (2010a) Late Oligocene-Miocene mid-latitude aridification and wind patterns in the Asian interior. Geology 38(6): 515–518. doi:10.1130/g30776.1

Sun Y, An Z, Clemens SC, Bloemendal J, Vandenberghe J (2010b) Seven million years of wind and precipitation variability on the Chinese Loess Plateau. Earth Planet Sci Lett 297:525–535. doi:10.1016/j.epsl.2010.07.004

Tada R (2004) Onset and evolution of millennial-scale variability in the Asian Monsoon and its impact on paleoceanography of the Japan Sea. In: Clift PD, Wang P, Hayes D (eds) Continent-Ocean Interactions in the East Asian Marginal Seas, AGU Monograph, vol 149., pp 255–282

Tada R, Irino T, Koizumi I (1999) Land-ocean linkages over orbital and millennial timescales recorded in late Quaternary sediments of the Japan Sea. Paleoceanography 14(2):236–247

Tada R, Zheng H, Sugiura N, Isozaki Y, Hasegawa H, Sun Y et al (2010) Desertification and dust emission history of the Tarim Basin and its relation to the uplift of northern Tibet. J Geol Soc Special Publications 342(1):45–65. doi:10.1144/sp342.5

Tada R, Murray RW, Alvarez Zarikian CA, The Expedition 346 Scientists (2015) Proc. IODP. Integrated Ocean Drilling Program, College Station, TX, p 346. doi:10.2204/iodp.proc.346.2015

Tang H, Micheels A, Eronen JT, Ahrens B, Fortelius M (2013) Asynchronous responses of East Asian and Indian summer monsoons to mountain uplift shown by regional climate modelling experiments. Clim Dyn 40(5–6):1531–1549. doi:10.1007/s00382-012-1603-x

Tapponnier P, Zhiqin X, Roger F, Meyer B, Arnaud N, Wittlinger G et al (2001) Oblique stepwise rise and growth of the Tibet plateau. Science 294(5547): 1671–1677. doi:10.1126/science.105978

Thiede RC, Sobel ER, Chen J, Schoenbohm LM, Stockli DF, Sudo M et al (2013) Late Cenozoic extension and crustal doming in the India-Eurasia collision zone: New thermochronologic constraints from the NE Chinese Pamir. Tectonics 32(3):763–779. doi:10.1002/tect.20050

Tripati AK, Roberts CD, Eagle RA (2009) Coupling of CO_2 and ice sheet stability over major climate transitions of the last 20 million years. Science 326(5958): 1394–1397. doi:10.1126/science.1178296

Wang L, Chen W (2014) An intensity index for the East Asian winter monsoon. J Clim 27:2361–2374

Wang L, Sarnthein M, Erlenkeuser H, Grimalt J, Grootes P, Heilig S et al (1999) East Asian monsoon climate during the Late Pleistocene: high-resolution sediment records from the South China Sea. Mar Geol 156:245–284

Wang Y, Cheng H, Edwards RL, Kong X, Shao X, Chen S et al (2008) Millennial- and orbital-scale changes in the East Asian monsoon over the past 224,000 years. Nature 451(7182):1090–1093. doi:10.1038/nature06692

Wang Y, Deng T, Flynn L, Wang X, Yin A, Xu Y et al (2012) Late Neogene environmental changes in the central Himalaya related to tectonic uplift and orbital forcing. J Asian Earth Sci 44:62–76. doi:10.1016/j.jseaes.2011.05.020

Wang P, Prell WL, Blum P, Leg184 Shipboard Scientific Party (2000) Proc. ODP Init Repts. Ocean Drilling Program, College Station, TX, p 184. doi:10.2973/odp.proc.ir.184.2000

Wara MW, Ravelo AC, Delaney ML (2005) Permanent El Nino-like conditions during the Pliocene warm period. Science 309(5735):758–761. doi:10.1126/science.1112596

Webb AAG (2013) Preliminary palinspastic reconstruction of Cenozoic deformation across the Himachal Himalaya (northwestern India). Geosphere 9:572–587

Webb AAG, Schmitt AK, He D, Weigand EL (2011) Structual and geochronological evidence for the leading edge of the Greater Himalayan Crystalline complex in the central Nepal Himalaya. Earth Planet Sci Lett 304:483–495

Webster PJ, Magana VO, Palmer TN, Shukla J, Tomas RA, Yanai M et al (1998) Monsoons: processes, predictability, and the prospects for prediction. J Geophys Res-Oceans 103(C7):14451–14510. doi:10.1029/97jc02719

Whipp DM, Ehlers TA, Blythe AE, Huntington KW, Hodges KV, Burbank DW (2007) Plio-Quaternary exhumation history of the central Nepalese Himalaya: 2. Thermokinematic and thermochronometer age prediction model. Tectonics 26(3):1–23. doi:10.1029/2006tc001991

Wu C, Nelson KD, Wortman G, Samson SD, Yue Y, Li J et al (1998) Yadong cross structure and South Tibetan Detachment in the east central Himalaya (89°-90°E). Tectonics 17(1):28–45. doi:10.1029/97tc03386

Wu F, Fang X, Ma Y, Herrmann M, Mosbrugger V, An Z et al (2007) Plio–Quaternary stepwise drying of Asia: evidence from a 3-Ma pollen record from the Chinese Loess Plateau. Earth Planet Sci Lett 257(1–2):160–169. doi:10.1016/j.epsl.2007.02.029

Wu G, Liu Y, Dong B, Liang X, Duan A, Bao Q et al (2012a) Revisiting Asian monsoon formation and change associated with Tibetan Plateau forcing: I. Formation Clim Dyn 39(5):1169–1181. doi:10.1007/s00382-012-1334-z
Wu G, Liu Y, He B, Bao Q, Duan A, Jin FF (2012b) Thermal controls on the Asian summer monsoon. Sci Rep 2(404):1–7. doi:10.1038/srep00404
Wu Z, Hu D, Ye P, Wu Z (2013) Early Cenozoic tectonics of the Tibetan Plateau. Acta Geologica Cinica 87(2):289–303
Xiao GQ, Abels HA, Yao ZQ, Dupont-Nivet G, Hilgen FJ (2010) Asian aridification linked to the first step of the Eocene-Oligocene climate Transition (EOT) in obliquity-dominated terrestrial records (Xining Basin, China). Clim Past 6(4): 501–513. doi:10.5194/cp-6-501-2010
Xiao G, Guo Z, Dupont-Nivet G, Lu H, Wu N, Ge J et al (2012) Evidence for northeastern Tibetan Plateau uplift between 25 and 20 Ma in the sedimentary archive of the Xining Basin, Northwestern China. Earth Planet Sci Lett 317–318:185–195. doi:10.1016/j.epsl.2011.11.008
Xu H, Chang F, Luo Y, Sun X (2009) Palaeoenvironmental changes from pollen record in deep sea core PC-1 from northern Okinawa Trough, East China Sea during the past 24 ka. Chin Sci Bull 54(20):3739–3748. doi:10.1007/s11434-009-0227-y
Xu WC, Zhang HF, Harris N, Guo L, Pan FB (2013) Rapid Eocene erosion, sedimentation and burial in the eastern Himalayan syntaxis and its geodynamic significance. Gondwana Res 23(2):715–725. doi:10.1016/j.gr.2012.05.011
Yanai M, Wu G (2006) Effects of the Tibetan Plateau. In: Wang B (ed) The Asian Monsoon. Praxis, Springer, Berlin, pp 513–549
Yasunari T, Saito K, Takata K (2006) Relative roles of large-scale orography and land surface processes in the global hydroclimate. Part I: impacts on monsoon systems and the tropics. J Hydrometeor 7:626–641
Yin A, Rumelhart PE, Butler R, Cowgill E, Harrison TM, Foster DA et al (2002) Tectonic history of the Altyn Tagh fault system in northern Tibet inferred from Cenozoic sedimentaion. Geol Soc Am Bull 114(10):1257–1295
Yuan DY, Ge WP, Chen ZW, Li CY, Wang ZC, Zhang HP et al (2013) The growth of northeastern Tibet and its relevance to large-scale continental geodynamics: A review of recent studies. Tectonics 32(5):1358–1370. doi:10.1002/tect.20081
Zachos J, Pagani M, Sloan L, Thomas E, Billups K (2001) Trends, rhythms, and aberrations in global climate 65 Ma to present. Science 292:686–693
Zhang R, Murphy MA, Lapen TJ, Sanchez V, Heizler M (2011) Late Eocene crustal thickening followed by early-late Oligocene extention along the India-Asia suture zone: evidence for cyclicity in the Himalayan orogen. Geosphere 7(5): 1249–1268. doi:10.1130/ges00643.1
Zhang R, Jiang D, Liu X, Tian Z (2012a) Modeling the climate effects of different subregional uplifts within the Himalaya-Tibetan Plateau on Asian summer monsoon evolution. Chin Sci Bull 57(35):4617–4626. doi:10.1007/s11434-012-5284-y
Zhang Z, Flatøy F, Wang H, Bethke I, Bentsen M, Guo Z (2012b) Early Eocene Asian climate dominated by desert and steppe with limited monsoons. J Asian Earth Sci 44:24–35. doi:10.1016/j.jseaes.2011.05.013
Zhang YG, Pagani M, Liu Z, Bohaty SM, DeConto R (2013) A 40-million-year history of atmospheric CO_2. Phil Trans R Soc A 371:20130096
Zhao P, Zhou Z (2009) An East Asian subtripical summer monsoon index and its relationship to summer rainfall in China. Acta Meteorol Sin 23:18–28
Zheng H, Powell CM, An Z, Zhou J, Dong G (2000) Pliocene uplift of the northern Tibetan Plateau. Geology 28(8):715–718
Zheng D, Zhang PZ, Wan JL, Yuan DY, Li CY, Yin GM GLZ et al (2006) Rapid exhumation at ~8 Ma on the Liupan Shan thrust fault from apatite fission-track thermochronology: implications for growth of the northeastern Tibetan Plateau margin. Earth Planet Sci Lett 248:198–208. doi:10.1016/j.epsl.2006.05.023
Zheng D, Clark MK, Zhang P, Zheng W, Farley KA (2010) Erosion, fault initiation and topographic growth of the North Qilian Shan (northern Tibetan Plateau). Geosphere 6(6):937–941. doi:10.1130/ges00523.1
Zheng H, Wei X, Tada R, Clift PD, Wang B, Jourdan F et al (2015) Late Oligocene-early Miocene birth of the Taklimakan desert. PNAS 112(25):7662–7667. doi:10.1073/pnas.1424487112
Zhu L, Wang C, Zheng H, Xiang F, Yi H, Liu D (2006) Tectonic and sedimentary evolution of basins in the northeast of Qinghai-Tibet Plateau and their implication for the northward growth of the Plateau. Palaeogeogr Palaeoclimatol Palaeoecol 241(1):49–60. doi:10.1016/j.palaeo.2006.06.019

Submit your manuscript to a SpringerOpen journal and benefit from:

► Convenient online submission
► Rigorous peer review
► Immediate publication on acceptance
► Open access: articles freely available online
► High visibility within the field
► Retaining the copyright to your article

Submit your next manuscript at ► springeropen.com